Table 5 Multivariate analysis of factors predictive of long-term survival in patients with HCC

Variable	Hazard ratio (95% CI)	*P* value
Age (years)	1.021 (0.997–1.046)	0.081
Gender (female/male)	0.759 (0.484–1.189)	0.229
HBsAg (negative/positive)	1.401 (0.712–2.759)	0.329
Anti-HCV (negative/positive)	0.916 (0.505–1.663)	0.774
Alcohol intake (not frequent/frequent)	0.740 (0.347–1.601)	0.451
Child–Pugh class (A/B, C)	2.269 (1.509–3.410)	<0.001
Log (AFP ng/ml)	1.310 (1.102–1.558)	0.002
μ-TAS AFP-L3 (<7/≥7)	1.673 (1.079–2.594)	0.021
Log (DCP mAU/ml)	1.220 (0.970–1.534)	0.089
Maximum tumor size (mm)	1.007 (0.994–1.012)	0.511
Tumor number (single/multiple)	2.297 (1.393–3.787)	0.001
Vessel invasion (negative/positive)	2.654 (1.265–5.566)	0.010
Treatment (hepatic resection/RFA, PEI, TACE, and TAI)	1.739 (1.093–2.767)	0.019

HCC hepatocellular carcinoma, *HBsAg* hepatitis B surface antigen, *HCV* hepatitis C virus, *AFP* alpha-fetoprotein, *AFP-L3* fucosylated fraction of AFP, *DCP* des-gamma-carboxy prothrombin, *μ-TAS* micro-total analysis system, *RFA* radiofrequency ablation, *PEI* percutaneous ethanol injection, *TACE* transcatheter arterial chemoembolization, *TAI* transcatheter arterial infusion chemotherapy, *CI* confidence interval. Hazard ratio and *P* values were calculated using Cox's proportional-hazard model

a 7% cutoff value was 2.7-fold (44.2% versus 16.3%) higher than for the LiBASys assay in 43 stage I HCC patients. The detection of early-stage HCC using the μ-TAS assay will increase the opportunity for curative treatment and improve the survival of patients with HCC.

In addition to this high analytical sensitivity, the μ-TAS assay requires only 10 min to determine AFP-L3%, and is a fully automated instrument platform [16]. This shortening of the assay time in comparison with the LiBASys assay, for which the runtime is about 1 h, contributes to its clinical convenience for outpatients with HCC, and will allow clinicians to detect HCC, making it possible to perform prompt imaging diagnosis using modalities such as CT and MRI.

A number of studies have shown that AFP-L3 status is an independent prognostic factor in patients with HCC [9–13]. We previously reported that patients with AFP-L3 positivity of more than 15% had an unfavorable survival rate in comparison with patients showing 15% or less for AFP-L3. Moreover, the differences were more significant in the subgroups with lower AFP concentrations [20]. We demonstrated that μ-TAS AFP-L3 status (<7% or ≥7%) was a factor significantly predictive of long-term survival in patients with HCC, and confirmed that the survival rate of patients with elevated μ-TAS AFP-L3 level (≥7%) was significantly lower than that of patients without such elevation.

In conclusion, the present study has demonstrated that the μ-TAS AFP-L3 value is more sensitive for discriminating HCC than is the conventional LiBASys AFP-L3. This diagnostic sensitivity was especially good in subgroups with lower AFP concentrations, and improved the clinical utility of AFP-L3 for detection of early-stage HCC. In addition, to maximize the utility of this high sensitivity, we suggest that a cutoff value of 7% is most appropriate for discriminating HCC from BLD using this newly developed μ-TAS AFP-L3 assay.

Acknowledgments This study was supported in part by a Grant-in-Aid (20390205), Japan Society for the Promotion Science, and a Grant-in-Aid from Health, Labor, and Welfare, Japan.

References

1. Abelev GI. Production of embryonal serum alpha-globulin by hepatoma: review of experimental and clinical data. *Cancer Res.* 1968;28:1344–1350.
2. Conor GI, Tatarinov YS, Abelev GI, Uriel J. A collaborative study for the evaluation of a serologic test for primary liver cancer. *Cancer.* 1970;25:1091–1098.
3. Bayati N, Silverman AL, Gordon SC. Serum alpha-fetoprotein levels and liver histology in patients with chronic hepatitis C. *Am J Gastroenterol.* 1998;93:2452–2456.
4. Goldstein NS, Blue DE, Hankin R, et al. Serum alpha-fetoprotein levels in patients with chronic hepatitis C. Relationships with serum alanine aminotransferase values, histologic activity index, and hepatocyte MIB-1 scores. *Am J Clin Pathol.* 1999;111:811–816.
5. Chu CW, Hwang SJ, Luo JC, et al. Clinical, virologic, and pathologic significance of elevated serum alpha-fetoprotein levels in patients with chronic hepatitis C. *J Clin Gastroenterol.* 2001;32:240–244.
6. Aoyagi Y, Suzuki Y, Isemura M, et al. The fucosylation index of alpha-fetoprotein and its usefulness in the early diagnosis of hepatocellular carcinoma. *Cancer.* 1988;61:769–774.
7. Aoyagi Y, Saitoh A, Suzuki Y, et al. Fucosylation index of alpha-fetoprotein, a possible aid in the early recognition of hepatocellular carcinoma in patients with cirrhosis. *Hepatology.* 1993;17:50–52.

8. Taketa K, Endo Y, Sekiya C, et al. A collaborative study for the evaluation of lectin-reactive alpha-fetoproteins in early detection of hepatocellular carcinoma. *Cancer Res.* 1993;53:5419–5423.
9. Aoyagi Y, Isokawa O, Suda T, et al. The fucosylation index of alpha-fetoprotein as a possible prognostic indicator for patients with hepatocellular carcinoma. *Cancer.* 1998;83:2076–2082.
10. Hayashi K, Kumada T, Nakano S, et al. Usefulness of measurement of Lens culinaris agglutinin-reactive fraction of alpha-fetoprotein as a marker of prognosis and recurrence of small hepatocellular carcinoma. *Am J Gastroenterol.* 1999;94:3028–3033.
11. Oka H, Saito A, Ito K, et al. Multicenter prospective analysis of newly diagnosed hepatocellular carcinoma with respect to the percentage of Lens culinaris agglutinin-reactive alpha-fetoprotein. *J Gastroenterol Hepatol.* 2001;16:1378–1383.
12. Tateishi R, Shiina S, Yoshida H, et al. Prediction of recurrence of hepatocellular carcinoma after curative ablation using three tumor markers. *Hepatology.* 2006;44:1518–1527.
13. Miyaaki H, Nakashima O, Kurogi M, Eguchi K, Kojiro M. Lens culinaris agglutinin-reactive alpha-fetoprotein and protein induced by vitamin K absence II are potential indicators of a poor prognosis: a histopathological study of surgically resected hepatocellular carcinoma. *J Gastroenterol.* 2007;42:962–968.
14. Nakamura K, Imajo N, Yamagata Y, et al. Liquid-phase binding assay of alpha-fetoprotein using a sulfated antibody for bound/free separation. *Anal Chem.* 1998;70:954–957.
15. Kawabata T, Wada HG, Watanabe M, Satomura S. Electrokinetic analyte transport assay for alpha-fetoprotein immunoassay integrates mixing, reaction and separation on-chip. *Electrophoresis.* 2008;29:1399–1406.
16. Kagebayashi C, Yamaguchi I, Akinaga A, et al. Automated immunoassay system for AFP-L3% using on-chip electrokinetic reaction and separation by affinity electrophoresis. *Anal Biochem.* 2009;388:306–311.
17. Liver Cancer Study Group of Japan. *The general rules for the clinical and pathological study of primary liver cancer, English edn.* Tokyo: Kanehara; 2003.
18. Kudo M, Chung H, Osaki Y. Prognostic staging system for hepatocellular carcinoma (CLIP score): its value and limitations, and a proposal for a new staging system, the Japan Integrated Staging Score (JIS score). *J Gastroenterol.* 2003;38:207–215.
19. Kumada T, Nakano S, Takeda I, et al. Clinical utility of Lens culinaris agglutinin-reactive alpha-fetoprotein in small hepatocellular carcinoma: special reference to imaging diagnosis. *J Hepatol.* 1999;30:125–130.
20. Kobayashi M, Kuroiwa T, Suda T, et al. Fucosylated fraction of alpha-fetoprotein, L3, as a useful prognostic factor in patients with hepatocellular carcinoma with special reference to low concentrations of serum alpha-fetoprotein. *Hepatol Res.* 2007;37:914–922.

Dig Dis Sci (2009) 54:2530–2537
DOI 10.1007/s10620-008-0642-y

ORIGINAL ARTICLE

Serum Alpha-Fetoprotein Levels During and After Interferon Therapy and the Development of Hepatocellular Carcinoma in Patients with Chronic Hepatitis C

Yasushi Tamura · Satoshi Yamagiwa · Yohei Aoki · So Kurita · Takeshi Suda · Shogo Ohkoshi · Minoru Nomoto · Yutaka Aoyagi · The Niigata Liver Disease Study Group

Received: 22 September 2008 / Accepted: 12 November 2008 / Published online: 18 December 2008

Abstract The association between serum alpha-fetoprotein (AFP) levels during and after interferon (IFN) therapy and the development of hepatocellular carcinoma (HCC) was evaluated in patients with chronic hepatitis C (CHC). A total of 263 patients treated by IFN with or without ribavirin were enrolled in the study. Serum AFP levels during and after IFN therapy were investigated retrospectively, and statistical analysis was performed to identify the factors associated with HCC development. During IFN therapy, serum AFP levels significantly decreased, regardless of virologic response to treatment. Increased serum AFP levels ($\geq$10 ng/ml) at the end of IFN therapy (EOT) was a close-to-significant variable affecting the development of HCC ($P = 0.057$), and a significantly higher cumulative incidence of HCC was seen in patients with increased serum AFP levels at EOT ($P = 0.021$). Serum AFP level at EOT is a possible predictor of HCC in CHC patients after IFN therapy.

Keywords Chronic hepatitis C · Interferon · Alpha-fetoprotein · Hepatocellular carcinoma

Introduction

Hepatitis C virus (HCV) has a worldwide prevalence. HCV infection frequently causes chronic liver disease leading to liver cirrhosis, and increases the risk of hepatocellular carcinoma (HCC) [1–5]. Interferon (IFN)-based therapy has been used in patients with chronic hepatitis C (CHC), as it has been shown not only to eradicate HCV but also to reduce serum alanine aminotransferase (ALT) levels [5–9]. Moreover, several studies have indicated that IFN therapy reduces the rate of development of HCC and results in improved survival in patients with CHC [10, 11]. Nevertheless, there have been many reports of the detection of HCC in some patients with CHC even after successful eradication of HCV by IFN therapy [12, 13]. Although several factors, such as older age, male gender, and severe fibrosis, have been implicated [12, 13], the factors associated with the development of HCC after IFN therapy are still inconclusive.

Alpha-fetoprotein (AFP), a 70-kDa single-stranded glycoprotein, has been widely used as a diagnostic marker for HCC [14, 15]. Although elevated serum AFP level in patients with CHC has been shown to be a significant independent predictor of the development of HCC [4, 5], AFP levels are sometimes elevated in patients with chronic hepatitis and cirrhosis who have no evidence of HCC [16–18]. Especially among patients with advanced CHC, serum AFP values are frequently elevated (e.g., at a rate of 47% in patients with cirrhosis), even in the absence of HCC [20]. Therefore, the usefulness of AFP as a screening marker of HCC has been limited by its impaired specificity. Several studies have revealed that elevation of serum AFP levels in CHC is associated with female gender, elevated serum ALT level, prolonged prothrombin time, decreased platelet count, low serum albumin level, hepatic necroinflammation and fibrosis in biopsy specimens, and genotype 1b HCV infection [18–22]. In addition, IFN therapy decreases serum AFP levels in patients with CHC [20–24]. However, there is little knowledge about the relationship between the

Y. Tamura (✉) · S. Yamagiwa · Y. Aoki · S. Kurita · T. Suda · S. Ohkoshi · M. Nomoto · Y. Aoyagi
Division of Gastroenterology and Hepatology, Graduate School of Medical and Dental Sciences, Niigata University, 757 Asahimachi-dori 1, Chuo-ku, Niigata 951-8510, Japan
e-mail: ytamura@med.niigata-u.ac.jp

The Niigata Liver Disease Study Group
The Niigata Liver Disease Study Group, Niigata, Japan

changes in serum AFP level associated with IFN therapy and the development of HCC. We therefore investigated the changes in serum AFP levels during and after IFN therapy, and we evaluated the clinical significance of changes in AFP value in the prediction of HCC development after IFN therapy.

Methods

Patients and Treatment

A total of 263 patients with CHC treated by IFN with or without ribavirin at hospitals participating in the Niigata Liver Disease Study Group from January 2000 to May 2007 were investigated retrospectively. All patients were confirmed to be seropositive for anti-HCV antibody and HCV-RNA. Patients with hepatitis B surface-antigen positivity, autoimmune hepatitis, or alcoholic liver disease, were excluded from the study. No patient had a previous history of treatment for HCC or had liver tumors detectable by ultrasound (US) or computed tomography (CT) before treatment. Histopathologic examinations before IFN therapy were performed in 174 patients. Hepatic inflammation and fibrosis of specimens were assessed according to the new Inuyama classification of chronic hepatitis in Japan [25]. There were four degrees of inflammation: A0 (no inflammation), A1 (mild), A2 (moderate), and A3 (severe). There were five degrees of fibrosis: F0 (no fibrosis), F1 (mild), F2 (moderate), F3 (severe), and F4 (cirrhosis). In accordance with approval of the study protocol by the institutional review board of Niigata University Medical and Dental Hospital, written informed consent was appropriately obtained from all of the individuals enrolled in the study. The study was carried out in accordance with the ethical guidelines of the 1975 Declaration of Helsinki.

The IFNs used in this study were pegylated-IFN (Peg-IFN) α-2b, Peg-IFNα-2a, recombinant IFNα-2b, consensus IFNα, and natural IFNα. Of the 263 patients, 114 (43.3%) were treated with Peg-IFNα-2b (1.5 μg/kg weekly) and ribavirin (600–1,000 mg daily); 71 (27.0%) were treated with recombinant IFNα-2b (6–10 MIU three times weekly) and ribavirin (600–1,000 mg daily); 61 (23.2%) were treated with Peg-IFNα-2a (90–180 μg weekly); ten (3.8%) were treated with consensus IFNα (9–18 MIU three times weekly); and seven (2.7%) were treated with natural IFNα (3–6 MIU two or three times weekly). Doses of IFNs and/or ribavirin were reduced when adverse effects, such as neutropenia or anemia, were observed. Most patients infected with genotype II HCV were treated for 24 weeks, and patients infected with genotype I HCV were usually treated for 48 weeks or more. All patients were followed for at least 24 more weeks after the end of treatment (EOT). Qualitative polymerase chain reaction (PCR) assay 24 weeks after the end of treatment was used to evaluate efficacy of treatment according to elimination of HCV-RNA. Patients were classified by virologic response into three groups: sustained virologic response (SVR), relapse, and no response (NR). SVR was defined as negative HCV-RNA 24 weeks after EOT. Relapse was defined as negative HCV-RNA during IFN therapy and positive HCV-RNA 24 weeks after EOT regardless of the serum ALT level. NR was defined as positive HCV-RNA during IFN therapy and 24 weeks after EOT.

Laboratory Examinations and Follow-Up

The white blood cell count, red blood cell count, platelet count, serum ALT level, and serum albumin level were measured before treatment (at baseline) and at least once every 4 weeks after initiation of treatment. Serum AFP level was measured before treatment and once every 1 to 6 months during the follow-up period. HCV-RNA was tested before treatment and 24 weeks after treatment by qualitative PCR assay (Amplicor HCV version 2.0; Roche Diagnostics Co., Tokyo, Japan), with a detection limit of 50 IU/ml. Viral (HCV-RNA) load was measured before and during treatment by quantitative PCR assay (Amplicor HCV monitor version 2.0; Roche Diagnostics Co., Tokyo, Japan) with a detection limit of 500 IU/ml. HCV-RNA genotype was determined by an immunoserological typing method (Immucheck F-HCV Gr Kokusai; Sysmex, Kobe, Japan). Besides laboratory examinations, patients were screened for the presence of HCC by several imaging modalities (US, CT, and magnetic resonance imaging). The status of patients enrolled in this study was confirmed as of November 2007.

Statistical Analysis

In accordance with their pretreatment AFP values, the 263 subjects were divided into two groups: a low AFP group (AFP <10 ng/ml; $n = 191$) and a high AFP group (AFP ≥10 ng/ml; $n = 72$). Differences in the distributions of clinical features between the two groups were determined by Fisher's exact test and the Mann–Whitney test. Logistic regression analysis was performed with forward selection to identify the factors associated with serum AFP level at baseline. Wilcoxon signed-rank test was used to compare the changes in serum AFP level from baseline to EOT and from EOT to 24 weeks after EOT. A Cox's proportional hazards model was used to analyze the factors contributing to development of HCC; factors examined were age, gender, ALT, platelet count, albumin, AFP, histopathologic findings (inflammation and fibrosis), HCV genotype, HCV load, duration of treatment, and efficacy of IFN (SVR vs.

relapse and NR). Cumulative development of HCC based on serum AFP level (<10 ng/ml vs. ≥10 ng/ml) at EOT was determined by the Kaplan–Meier method. Differences between the curves were evaluated by log-rank test. Statistical analyses were performed by SPSS 15.0 (SPSS Japan Inc., Tokyo, Japan). A *P*-value of <0.05 was considered statistically significant.

Results

Clinical Features of Patients Classified by Serum AFP Level at Baseline

A total of 263 patients were studied. The mean AFP level (mean ± SD) at baseline was 15.0 ± 41.9 ng/ml, and the median was 5.1 ng/ml (range, 1.0–542.0). There were 71 patients with serum AFP ≥10 ng/ml at baseline (27.0%). The serum AFP level usually remained elevated without large fluctuations, although the evident pattern of AFP elevation varied in each patient. Clinical features of patients classified by serum AFP level (<10 ng/ml vs. ≥10 ng/ml) at baseline are shown in Table 1. Patients with elevated AFP (≥10 ng/ml) were characterized by older age ($P < 0.001$), high ALT level ($P < 0.001$), low platelet count ($P < 0.001$), low albumin level ($P < 0.001$), and progression of hepatic inflammation ($P < 0.001$) and fibrosis ($P < 0.001$). No significant difference was seen in gender, HCV genotype, or HCV-RNA viral load. Multivariate logistic regression analysis revealed that the factors correlated with elevated serum AFP at baseline were low serum albumin level ($P = 0.001$) and severe hepatic inflammation ($P = 0.02$) (Table 2).

Changes in Serum AFP Level During and After IFN Therapy

Mean duration of IFN therapy was 39.6 ± 16.5 weeks. One hundred thirty-two (50.2%) patients were treated for 24 to 47 weeks, and 131 (49.8%) were treated for 48 or more weeks. Of the 263 patients treated with IFNs, 136 (51.7%) were defined as SVR, 51 (19.4%) as relapse, and 76 (28.9%) as NR. Serum AFP levels decreased gradually during IFN therapy without fluctuations, and a significant decrease was observed regardless of response to treatment. ($P < 0.001$, $P = 0.003$, and $P < 0.001$ for SVR, relapse, and NR, respectively). In the SVR group, a decrease in serum AFP level was also observed after treatment ($P = 0.037$) (Table 3). The significant decrease of serum AFP level was not associated with hepatic fibrosis, as seen in both patients with mild (F0-2) ($P < 0.001$) and severe hepatic fibrosis (F3 and F4) ($P = 0.012$) (Table 4).

Next, we evaluated the changes in serum AFP level according to the treatment regimens. Among patients treated with Peg-IFNα-2b, recombinant IFNα-2b and Peg-IFNα-2a, the decrease in the serum AFP level during IFN therapy was not associated with the treatment regimen ($P < 0.001$, $P < 0.001$ and $P = 0.001$, for Peg-IFNα-2b

Table 1 Clinical features of patients classified by serum AFP level at baseline

Characteristics	AFP <10 ng/ml ($n = 191$)	AFP ≥10 ng/ml ($n = 72$)	*P*-value
Age (years)	54.3 ± 11.8	60.0 ± 8.6	<0.001
Gender (Female/Male)	84/107	41/31	0.072
ALT (IU/l)	85.8 ± 88.1	104.5 ± 66.3	<0.001
Platelet ($\times 10^4$/μl)	16.8 ± 5.6	13.1 ± 4.8	<0.001
Albumin (g/dl)	4.4 ± 0.3	4.0 ± 0.5	<0.001
Histopathology			
Inflammation (A0-1/A2-3)	68/57	7/42	<0.001
Fibrosis (F0-2/F3-4)	116/9	30/19	<0.001
HCV-RNA			
Serology (Group 1/2)	131/57	54/18	0.446
Viral load			
(0-99/100-499/500 < KIU/ml)	18/39/99	8/16/30	0.588

ALT alanine aminotransferase, *AFP* alpha-fetoprotein, *HCV* hepatitis C virus. Values are expressed as mean ± SD

Table 2 Multivariate logistic regression analysis for predicting elevated AFP (≥10 ng/ml) at baseline

Variables	Coefficient	SE	OR (95% CI)	*P*-value
Albumin (g/dl)	−2.502	0.724	0.082 (0.020–0.339)	0.001
Inflammation (A0-1/A2-3)	1.525	0.656	4.594 (1.270–16.617)	0.020

SE standard error, *OR* odds ratio, *CI* confidence interval

Table 3 Changes in serum AFP level during and after IFN therapy according to the virologic response

Virological response	Baseline	EOT	24 weeks after EOT
SVR			
Median AFP (ng/ml)	4.2	3.4*	3.3†
(range)	(1.0–153.0)	(1.0–12.9)	(1.0–10.3)
Relapse			
Median AFP (ng/ml)	5.8	4.1**	3.9
(range)	(1.0–271.8)	(2.0–31.6)	(1.0–82.7)
NR			
Median AFP (ng/ml)	8.3	5.9*	6.0
(range)	(1.5–542.0)	(1.5–59.8)	(1.3–109.0)

Wilcoxon signed-ranks test was used. * $P < 0.001$, compared to baseline; ** $P = 0.003$, compared to baseline; † $P = 0.037$, compared to EOT

AFP alpha-fetoprotein, *SVR* sustained virologic response, *NR* non-response, *EOT* end of treatment

Table 4 Changes in serum AFP level during and after IFN therapy according to the hepatic fibrosis

Hepatic fibrosis	Baseline	EOT	24 weeks after EOT
Slight fibrosis, F0-2			
Median AFP (ng/ml)	4.4	3.5*	3.3
(range)	(1.0–153.0)	(1.0–59.8)	(1.0–37.4)
Advanced fibrosis, F3-4			
Median AFP (ng/ml)	14.1	6.5**	6.3
(range)	(2.6–542.0)	(1.5–54.4)	(1.8–82.7)

Wilcoxon signed-ranks test was used. * $P < 0.001$, compared to baseline; ** $P = 0.012$, compared to baseline

AFP alpha-fetoprotein, *EOT* end of treatment

and ribavirin, recombinant IFNα-2b and ribavirin, Peg-IFNα-2a, respectively) (Table 5). We were unable to evaluate the changes in serum AFP level in patients treated with consensus IFNα or natural IFNα owing to the small number of cases.

Risk Factors for Development of HCC

The mean observation period from initiation of IFN therapy was 162.4 ± 82.3 weeks (range, 89.7–367.7). HCC developed in seven patients within the study period. The final diagnosis of HCC was determined by imaging modalities. Two of the seven were patients defined as SVR and five as NR. The mean length of time from initiation of IFN therapy to diagnosis of HCC was 129.0 ± 77.3 weeks. Serum AFP levels at diagnosis of HCC were 2.2, 3.0, 4.0, 10.9, 11.9, 17.4, and 47.0 ng/ml. Of these seven patients, one showed F3 fibrosis, two were diagnosed clinically as having cirrhosis, and the other four were diagnosed as having chronic hepatitis at the start of IFN treatment. In the follow-up period from EOT to diagnosis of HCC, a pattern of AFP increase, a stable AFP pattern and a pattern of AFP decrease were seen in three, three and one patients, respectively (data not shown). Table 6 represents the changes in serum AFP level during and after IFN therapy in the patients who developed HCC and in those who did not. Univariate Cox's regression analysis revealed that older age at the initiation of therapy ($P = 0.038$) was a significant prognostic indicator of the development of HCC after IFN therapy, and increased serum AFP levels at EOT ($P = 0.057$) was a close-to-significant variable (Table 7). We examined the cumulative incidence of HCC development on the basis of serum AFP level (<10 ng/ml vs. ≥10 ng/ml) at EOT (Fig. 1). Patients with AFP ≥10 ng/ml had a significantly higher incidence of HCC than did those with AFP <10 ng/ml by log-rank test ($P = 0.021$).

Table 5 Changes in serum AFP level during and after IFN therapy according to the treatment regimens

Treatment regimens	Baseline	EOT	24 weeks after EOT
Peg-IFN α-2b + RBV			
Median AFP (ng/ml)	5.0	3.9*	4.0
(range)	(1.4–77.8)	(1.5–22.2)	(1.4–26.3)
Rec-IFN α-2b + RBV			
Median AFP (ng/ml)	7.3	4.1*	4.0
(range)	(1.0–542.0)	(1.0–54.4)	(1.0–35.1)
Peg-IFN α-2a			
Median AFP (ng/ml)	4.0	3.8**	3.5
(range)	(1.0–271.8)	(1.5–31.6)	(1.0–82.7)

Wilcoxon signed-ranks test was used. * $P < 0.001$, compared to baseline; ** $P = 0.001$, compared to baseline

AFP alpha-fetoprotein, *Peg-IFN* pegylated-IFN, *Rec-IFN* recombinant IFN, *RBV* Ribavirin, *EOT* end of treatment

Table 6 Changes in serum AFP level during and after IFN therapy in those with patients who developed HCC and in those without HCC

Patients	Baseline	EOT	24 weeks after EOT
Patients developed HCC			
Median AFP (ng/ml)	8.5	17.9	7.6
(range)	(3.6–61.0)	(2.2–46.0)	(1.0–109.0)
Patients without HCC			
Median AFP (ng/ml)	5.1	3.9*	3.9
(range)	(1.0–542.0)	(1.5–59.8)	(1.0–82.7)

Wilcoxon signed-ranks test was used. * $P < 0.001$, compared to baseline

AFP alpha-fetoprotein, *EOT* end of treatment

Table 7 Factors associated with the development of HCC after IFN therapy by univariate Cox's regression analysis

Variables	HR (95% CI)	*P*-value
Pre-treatment baseline variables		
Age (years)	1.117 (1.006–1.239)	0.038
Gender (Female/Male)	1.888 (0.365–9.772)	0.449
ALT (IU/l)	0.996 (0.984–1.009)	0.570
AFP (ng/ml)	0.998 (0.980–1.017)	0.856
Platelet ($\times 10^4/\mu l$)	0.956 (0.830–1.102)	0.539
Albumin (g/dl)	1.569 (0.159–15.518)	0.700
Histopathology		
Inflammation (A0-1/A2-3)	0.624 (0.086–4.521)	0.641
Fibrosis (F0-2/F3-4)	1.362 (0.137–13.558)	0.792
HCV-RNA		
Serology (Group 1/2)	1.195 (0.231–6.187)	0.832
Viral load (0-99/100-499/500 < KIU/ml)	1.422 (0.346–5.849)	0.625
Duration of therapy (week)	0.997 (0.919–1.038)	0.453
Efficacy of IFN (SVR/Relapse/NR)	2.453 (0.476–12.652)	0.284
Post-treatment variables at EOT		
ALT (IU/l)	1.006 (0.998–1.014)	0.137
AFP (ng/ml)	1.048 (0.999–1.101)	0.057
Platelet ($\times 10^4/\mu l$)	1.020 (0.889–1.171)	0.777
Albumin (g/dl)	0.115 (0.005–2.776)	0.183

HR hazard ratio, *CI* confidence interval, *ALT* alanine aminotransferase, *AFP* alpha-fetoprotein, *HCV* hepatitis C virus, *SVR* sustained virologic response, *NR* non-response, *EOT* end of treatment

Discussion

Until now, there has been little information on the relationship between the changes in serum AFP level associated with IFN therapy and the development of HCC, although several reports have described the changes in serum AFP level during IFN therapy. Consistent with our results, Murashima et al. [21] have already reported that IFN reduces the serum AFP level during treatment regardless of virologic response. Nomura et al. [23] also showed a significant decrease in serum AFP level during low-dose and long-term IFN monotherapy in 44 aged patients with CHC; SVR status was achieved in only two. In contrast, Chen et al. [22] demonstrated a significant decrease in serum AFP level during and after IFN therapy in an SVR group ($n = 26$), whereas no significant decrease in serum AFP level was observed in the non-SVR group ($n = 9$). The association of changes in serum AFP level during IFN therapy with the development of HCC was not examined in these studies.

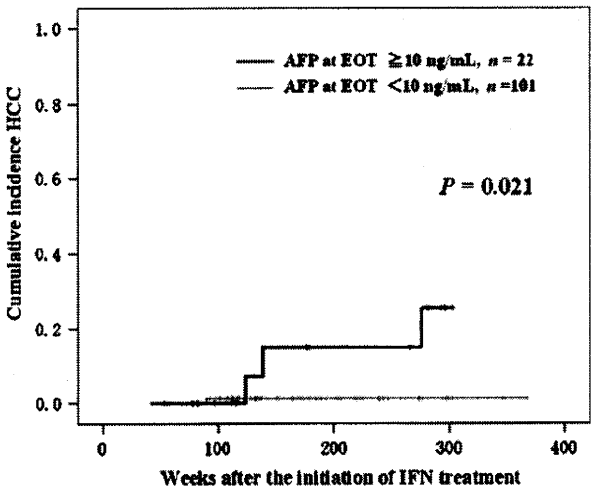

Fig. 1 Cumulative incidence HCC in two groups (serum AFP level <10 ng/ml, $n = 101$; vs. ≥10 ng/ml, $n = 22$) at the end of treatment. The high AFP group had a significantly higher incidence of HCC ($P = 0.021$). *AFP* alpha-fetoprotein, *EOT* end of treatment

We demonstrated that the serum AFP level in patients with CHC decreased during IFN therapy regardless of virologic response, and that, by univariate Cox's regression analysis, AFP level at EOT was a close-to-significant prognostic factor affecting the development of HCC. Moreover, a significantly higher cumulative incidence of HCC was seen in patients with increased serum AFP levels at EOT by log-rank test. Our results suggest that serum AFP level at EOT is a possible predictor of HCC development after IFN therapy and will be useful for considering additional treatments, such as long-term administration of low-dose IFN, to prevent HCC development.

AFP is a fetal glycoprotein produced by the yolk sac and fetal liver. Following birth, AFP is replaced by albumin as the major serum protein, and then the AFP level decreases rapidly. Consequently, AFP is not detectable in the sera of adults. However, production of AFP in adults occurs during liver regeneration and hepatocarcinogenesis. Therefore,

AFP has been used as a diagnostic marker for HCC [14, 15], although AFP levels are sometimes elevated in patients with chronic hepatitis and cirrhosis who have no evidence of HCC [16–18]. The reported prevalence of elevated AFP in patients with CHC varies from 10 to 43% [18, 19, 26, 27]. This wide discrepancy among previous reports is probably due to differences in the definition of elevated AFP value, as well as in patient population, ethnicity, and sample size. Chu et al. [18] reported that 28.7% (33/115) of patients with CHC had an elevated serum AFP level (≥12 ng/ml). Chen et al. [22] also reported that an elevated AFP level (≥10 ng/ml) was seen in 33% (41/123) of patients with CHC. Our results revealed that 27.0% (72/263) of patients with CHC had an elevated serum AFP level (≥10 ng/ml). This result is consistent with those of previous reports from Asian countries [18, 22].

Our multivariate logistic regression analysis revealed that hepatic inflammation and serum albumin level were significant independent factors associated with serum AFP level at baseline. Consistent with our results, several reports have shown that serum AFP level is correlated with the degree of hepatic inflammation in liver biopsy specimens [20]. Moreover, a number of studies have shown a relationship between elevated serum AFP level and decreased serum albumin level in patients with CHC [18, 21]. One of the reasons for these associations is simply the fact that advanced liver damage results in decreased production of albumin. In addition, reciprocal changes in albumin and AFP gene transcription during liver regeneration may account for the relationship between elevated serum AFP level and decreased serum albumin level [28, 29]. Although advanced hepatic fibrosis has been reported as the most common cause of serum AFP elevation [18, 22], our multivariate analysis was unable to demonstrate any association between serum AFP level and advanced hepatic fibrosis. In the present study, however, stage 3–4 fibrosis was significantly more frequent in the group showing elevated serum AFP levels. Moreover, the association of an elevated AFP level with a low albumin level may be secondary to a decrease of liver synthetic function due to cirrhosis. We speculated that one of the reasons for the discrepancy might be the fact that only 49 patients with an elevated serum AFP level underwent liver biopsy.

Many reports have described elevated serum AFP level, together with age, gender, and liver histologic stage, as independent risk factors for HCC in patients with CHC [4, 5]. Our results revealed that the hepatic inflammation was a significant independent factor associated with serum AFP level at baseline. These results indicate that active inflammation in the liver is one of the most important factors influencing serum AFP level, and suggest that this persistent inflammation results in hepatocarcinogenesis. In contrast, a number of reports have revealed that AFP itself can enhance the proliferation of mammalian tumor cells. Wang and Xu et al. [30] have reported that human AFP increases the proliferation of mouse H-22 hepatoma cells, and that the growth stimulatory activity of AFP could be abolished by anti-AFP antibodies. Wang and Xie et al. [31] showed that AFP enhances the proliferation of human HCC cells, and they suggested that this effect was mediated by an AFP/receptor autocrine pathway. In addition, AFP stimulates the expression of some oncogenes in human HCC cells and has immunosuppressive activity [32, 33]. These results suggest that not only hepatic inflammation accompanied by elevation of serum AFP level, but AFP itself, is associated with hepatocarcinogenesis.

Our univariate Cox's regression analysis revealed that serum AFP level at EOT was a close-to-significant prognostic variable affecting the development of HCC, although serum AFP level before treatment was not. Consistent with these results, Arase et al. [24] reported that in patients with CHC who were treated with IFN or herbal medicine, elevated serum AFP level (>10 ng/ml) after treatment was a statistically significant independent prognostic factor in the development of HCC. There are some factors other than AFP that could have a potential association with the development of HCC. Several studies have implicated obesity, diabetes, intake of alcohol, and smoking, as risk factors for HCC [34–37]. However, we did not investigate these factors in the present retrospective study. In addition, we were unable to exclude the possibility of occult HBV infection in patients with HCC, although all patients were negative for HBsAg.

In conclusion, our results revealed that serum AFP level decreased during IFN therapy regardless of the virologic response. In addition, serum AFP level at EOT was a close-to-significant prognostic factor for HCC development. These results suggest that serum AFP level at EOT should be utilized in making decisions on additional therapeutic options, such as long-term administration of low-dose IFN, to reduce the risk of HCC development in patients in whom HCV elimination by routine IFN therapy has failed. We realize our study has some limitations as follows: first, it was a retrospective analysis; second, various kinds of IFN were used; and third, the duration of IFN therapy varied from 24 to 90 weeks. Further prospective studies in which patients are treated by the current standard protocol-Peg-IFN with ribavirin-for a set period of time will confirm the relationship between changes in serum AFP level associated with IFN therapy and the development of HCC.

Acknowledgments The following doctors at each of the institutions participating in the Niigata Liver Disease Study Group contributed equally to the study: Nobuo Waguri and Kentaro Igarashi (Niigata City General Hospital, Niigata), Toru Ishikawa and Tomoteru Kamimura (Saiseikai Niigata Second Hospital, Niigata), Motoya Sugiyama (Niigata Prefectural Shibata Hospital, Shibata), Soichi Sugitani

(Tachikawa General Hospital, Nagaoka), Norio Ogata (Tsubame Rosai Hospital, Tsubame), Toru Hatano (Nagaoka Chuo General Hospital, Nagaoka), Toru Takahashi (Nagaoka Red Cross Hospital, Nagaoka), Hitoshi Bannai (Saiseikai Sanjo Hospital, Sanjo), Hiroto Wakabayashi (Takeda General Hospital, Aizuwakamatsu), Atsuo Sekine (Niigata Prefectural Yoshida Hospital, Tsubame), Toshiyuki Kato (Niigata Prefectural Cancer Center Hospital, Niigata), Masaaki Hirano (Niigata Prefectural Central Hospital, Joetsu), and Toru Miyajima (Toyosaka Hospital, Niigata).

References

1. Bruix J, Barrera JM, Calvet X, et al. Prevalence of antibodies to hepatitis C virus in Spanish patients with hepatocellular carcinoma and hepatic cirrhosis. *Lancet*. 1989;334:1004–1046. doi:10.1016/S0140-6736(89)91015-5.
2. Colombo M, Kuo G, Choo QL, et al. Prevalence of antibodies to hepatitis C virus in Italian patients with hepatocellular carcinoma. *Lancet*. 1989;334:1006–1008. doi:10.1016/S0140-6736(89)91016-7.
3. Hasan F, Jeffers LJ, De Medina M, et al. Hepatitis C-associated hepatocellular carcinoma. *Hepatology*. 1990;12:589–591. doi:10.1002/hep.1840120323.
4. Ikeda K, Saitoh S, Koida I, et al. A multivariate analysis of risk factors for hepatocellular carcinogenesis: a prospective observation of 795 patients with viral and alcoholic cirrhosis. *Hepatology*. 1993;18:47–53.
5. Tsukuma H, Hiyama T, Tanaka S, et al. Risk factors for hepatocellular carcinoma among patients with chronic liver disease. *N Engl J Med*. 1993;328:1797–1801. doi:10.1056/NEJM199306243282501.
6. Davis GL, Balart LA, Schiff ER, et al. Treatment of chronic hepatitis C with recombinant interferon alfa. A multicenter randomized, controlled trial. Hepatitis Interventional Therapy Group. *N Engl J Med*. 1989;321:1501–1506.
7. Di Bisceglie AM, Martin P, Kassianides C, et al. Recombinant interferon alfa therapy for chronic hepatitis C. A randomized, double-blind, placebo-controlled trial. *N Engl J Med*. 1989;321:1506–1510.
8. Causse X, Godinot H, Chevallier M, et al. Comparison of 1 or 3 MU of interferon alfa-2b and placebo in patients with chronic non-A, non-B hepatitis. *Gastroenterology*. 1991;101:497–502.
9. Chayama K, Saitoh S, Arase Y, et al. Effect of interferon administration on serum hepatitis C virus RNA in patients with chronic hepatitis C. *Hepatology*. 1991;13:1040–1043.
10. Nishiguchi S, Kuroki T, Nakatani S, et al. Randomised trial of effects of interferon-alpha on incidence of hepatocellular carcinoma in chronic active hepatitis C with cirrhosis. *Lancet*. 1995;346:1051–1055. doi:10.1016/S0140-6736(95)91739-X.
11. Ikeda K, Saitoh S, Arase Y, et al. Effect of interferon therapy on hepatocellular carcinogenesis in patients with chronic hepatitis type C: a long-term observation study of 1, 643 patients using statistical bias correction with proportional hazard analysis. *Hepatology*. 1999;29:1124–1130. doi:10.1002/hep.510290439.
12. Makiyama A, Itoh Y, Kasahara A, et al. Characteristics of patients with chronic hepatitis C who develop hepatocellular carcinoma after a sustained response to interferon therapy. *Cancer*. 2004;101:1616–1622. doi:10.1002/cncr.20537.
13. Ikeda M, Fujiyama S, Tanaka M, et al. Risk factors for development of hepatocellular carcinoma in patients with chronic hepatitis C after sustained response to interferon. *J Gastroenterol*. 2005;40:148–156. doi:10.1007/s00535-004-1519-2.
14. Abelev GI. Production of embryonal serum alpha-globulin by hepatoma: review of experimental and clinical data. *Cancer Res*. 1968;28:1344–1350.
15. Conor GI, Tatarinov YS, Abelev GI, Uriel J. A collaborative study for the evaluation of a serologic test for primary liver cancer. *Cancer*. 1970;25:1091–1098. doi:10.1002/1097-0142(197005)25:5<1091::AID-CNCR2820250514>3.0.CO;2-P.
16. Bayati N, Silverman AL, Gordon SC. Serum alpha-fetoprotein levels and liver histology in patients with chronic hepatitis C. *Am J Gastroenterol*. 1998;93:2452–2456. doi:10.1111/j.1572-0241.1998.00703.x.
17. Goldstein NS, Blue DE, Hankin R, et al. Serum alpha-fetoprotein levels in patients with chronic hepatitis C. Relationships with serum alanine aminotransferase values, histologic activity index, and hepatocyte MIB-1 scores. *Am J Clin Pathol*. 1999;111:811–816.
18. Chu CW, Hwang SJ, Luo JC, et al. Clinical, virologic, and pathologic significance of elevated serum alpha-fetoprotein levels in patients with chronic hepatitis C. *J Clin Gastroenterol*. 2001;32:240–244. doi:10.1097/00004836-200103000-00014.
19. Hu KQ, Kyulo NL, Lim N, Elhazin B, Hillebrand DJ, Bock T. Clinical significance of elevated alpha-fetoprotein (AFP) in patients with chronic hepatitis C, but not hepatocellular carcinoma. *Am J Gastroenterol*. 2004;99:860–865. doi:10.1111/j.1572-0241.2004.04152.x.
20. Di Bisceglie AM, Sterling RK, Chung RT, et al. HALT-C Trial group: serum alpha-fetoprotein levels in patients with advanced hepatitis C: results from the HALT-C Trial. *J Hepatol*. 2005;43:434–441. doi:10.1016/j.jhep.2005.03.019.
21. Murashima S, Tanaka M, Haramaki M, et al. A decrease in AFP level related to administration of interferon in patients with chronic hepatitis C and a high level of AFP. *Dig Dis Sci*. 2006;51:808–812. doi:10.1007/s10620-006-3211-2.
22. Chen TM, Huang PT, Tsai MH, et al. Predictors of alpha-fetoprotein elevation in patients with chronic hepatitis C, but not hepatocellular carcinoma, and its normalization after pegylated interferon alfa 2a-ribavirin combination therapy. *J Gastroenterol Hepatol*. 2007;22:669–675.
23. Nomura H, Kashiwagi Y, Hirano R, et al. Efficacy of low-dose long-term interferon monotherapy in aged patients with chronic hepatitis C genotype 1 and its relation to alpha-fetoprotein: a pilot study. *Hepatol Res*. 2007;37:490–497. doi:10.1111/j.1872-034X.2007.00073.x.
24. Arase Y, Suzuki F, Suzuki Y, et al. Prolonged-efficacy of bisphosphonate in postmenopausal women with osteoporosis and chronic liver disease. *J Med Virol*. 2008;80:1302–1307. doi:10.1002/jmv.21195.
25. Ichida F, Tsuji T, Omata M, et al. New Inuyama Classification; new criteria for histological assessment of chronic hepatitis. *Int Hepatol Commun*. 1996;6:112–119. doi:10.1016/S0928-4346(96)00325-8.
26. Fattovich G, Giustina G, Degos F, et al. Morbidity and mortality in compensated cirrhosis type C: a retrospective follow-up study of 384 patients. *Gastroenterology*. 1997;112:463–472. doi:10.1053/gast.1997.v112.pm9024300.
27. Sato Y, Nakata K, Kato Y, et al. Early recognition of hepatocellular carcinoma based on altered profiles of alpha-fetoprotein. *N Engl J Med*. 1993;328:1802–1806. doi:10.1056/NEJM199306243282502.
28. Niwa Y, Matsumura M, Shiratori Y, et al. Quantitation of alpha-fetoprotein and albumin messenger RNA in human hepatocellular carcinoma. *Hepatology*. 1996;23:1384–1392.
29. Panduro A, Shalaby F, Weiner FR, Biempica L, Zern MA, Shafritz DA. Transcriptional switch from albumin to alpha-fetoprotein and changes in transcription of other genes during carbon tetrachloride induced liver regeneration. *Biochemistry*. 1986;25:1414–1420. doi:10.1021/bi00354a034.
30. Wang XW, Xu B. Stimulation of tumor-cell growth by alpha-fetoprotein. *Int J Cancer*. 1998;75:596–599. doi:10.1002/(SICI)1097-0215(19980209)75:4<596::AID-IJC17>3.0.CO;2-7.

31. Wang XW, Xie H. Alpha-fetoprotein enhances the proliferation of human hepatoma cells in vitro. *Life Sci.* 1999;64:17–23. doi: 10.1016/S0024-3205(98)00529-3.
32. Li MS, Li PF, Chen Q, Du GG, Li G. Alpha-fetoprotein stimulated the expression of some oncogenes in human hepatocellular carcinoma Bel 7402 cells. *World J Gastroenterol.* 2004;10: 819–824.
33. Li MS, Ma QL, Chen Q, et al. Alpha-fetoprotein triggers hepatoma cells escaping from immune surveillance through altering the expression of Fas/FasL and tumor necrosis factor related apoptosis-inducing ligand and its receptor of lymphocytes and liver cancer cells. *World J Gastroenterol.* 2005;11:2564–2569.
34. Chen CL, Yang HI, Yang WS, et al. Metabolic factors and risk of hepatocellular carcinoma by chronic hepatitis B/C infection: a follow-up study in Taiwan. *Gastroenterology.* 2008;135:111–121. doi:10.1053/j.gastro.2008.03.073.
35. Hassan MM, Hwang LY, Hatten CJ, et al. Risk factors for hepatocellular carcinoma: synergism of alcohol with viral hepatitis and diabetes mellitus. *Hepatology.* 2002;36:1206–1213. doi: 10.1053/jhep.2002.36780.
36. Yuan JM, Govindarajan S, Arakawa K, Yu MC. Synergism of alcohol, diabetes, and viral hepatitis on the risk of hepatocellular carcinoma in blacks and whites in the US. *Cancer.* 2004;101: 1009–1017. doi:10.1002/cncr.20427.
37. Chiba T, Matsuzaki Y, Abei M, et al. The role of previous hepatitis B virus infection and heavy smoking in hepatitis C virus-related hepatocellular carcinoma. *Am J Gastroenterol.* 1996;91: 1195–1203.

Carcinogenesis vol.31 no.3 pp.504–511, 2010
doi:10.1093/carcin/bgp313
Advance Access publication December 16, 2009

IQGAP1 and vimentin are key regulator genes in naturally occurring hepatotumorigenesis induced by oxidative stress

Akihito Tsubota*, Kenji Matsumoto[1], Kaoru Mogushi[2], Koichi Nariai, Yoshihisa Namiki, Sadayori Hoshina, Hiroshi Hano[3], Hiroshi Tanaka[2], Hirohisa Saito[1] and Norio Tada

Institute of Clinical Medicine and Research, Jikei University School of Medicine, 163-1 Kashiwa-shita, Kashiwa, Chiba 277-8567, Japan, [1]Department of Allergy and Immunology, National Research Institute for Child Health and Development, 2-10-1 Okura, Setagaya-ku, Tokyo 157-8535, Japan, [2]Information Center for Medical Sciences, Tokyo Medical and Dental University, 1-5-45 Yushima, Bunkyo-ku, Tokyo 113-8510, Japan and [3]Department of Pathology, Jikei University School of Medicine, 3-25-8 Nishi-Shimbashi, Minato-ku, Tokyo 105-8461, Japan

*To whom correspondence should be addressed. Tel: +81 4 7164 1111 ext. 6601; Fax: +81 4 7166 8638;
Email: atsubo@jikei.ac.jp

To identify key genes involved in the complex multistep process of hepatotumorigenesis, we reduced multivariate clinicopathological variables by using the Long–Evans Cinnamon rat, a model with naturally occurring and oxidative stress-induced hepatotumorigenesis. Gene expression patterns were analyzed serially by profiling liver tissues from rats of a naive status (4 weeks old), through to those with chronic hepatitis (26 and 39 weeks old) to tumor development (67 weeks old). Of 31 099 probe sets used for microarray analysis, 87 were identified as being upregulated in a stepwise manner during disease progression and tumor development. Quantitative real-time reverse transcription–polymerase chain reaction and statistical analyses verified that IQGAP1 and vimentin mRNA expression levels increased significantly throughout hepatotumorigenesis. A hierarchical clustering algorithm showed both genes clustered together and in the same cluster group. Immunohistochemical and western blot analyses showed similar increases in protein levels of IAGAP1 and vimentin. Finally, pathway analyses using text-mining technology with more comprehensive and recent gene–gene interaction data identified IQGAP1 and vimentin as important nodes in underlying gene regulatory networks. These findings enhance our understanding of the multistep hepatotumorigenesis and identification of target molecules for novel treatments.

Introduction

Primary liver cancer ranks third worldwide as a cause for cancer-related mortality, according to World Health Organization reports. The incidence is increasing even in low-endemic Western countries, with hepatocellular carcinoma (HCC) and cholangiocarcinoma accounting for most of these cases. The prognosis for advanced liver cancer remains very poor.

Recent advances in microarray technology have resulted in exponential accumulation of gene expression profiling data and provided novel insights into the molecular mechanisms underlying hepatotumorigenesis (1–3). Nevertheless, the molecular pathogenesis of liver cancer is difficult to establish, because patients present with highly variable clinicopathological features, the risk factors are diverse and liver cancer is heterogenous in nature, both pathologically and biologically (4–7). Such heterogeneity and variation probably underlies the genomic diversity of liver cancer, making it difficult to identify gene signatures in hepatotumorigenesis. In fact, gene expression profiling patterns of HCC differ even between patients with hepatitis B and C virus infections (8,9). Alternatively, it is unclear whether differences in gene expression between tumor and non-tumor tissues represent the cause or consequence of the neoplastic transformation because liver cancer generally evolves through multistep and diverse dysregulated molecular pathways (4).

Liver cancer of any etiology is commonly preceded by chronic inflammation, which is linked tightly to oxidative stress (4,10,11). Indeed, oxidative stress is an important fundamental factor in tumorigenesis that is common to wide-ranging etiologies. For instance, oxidative stress promotes fibrogenesis, serves as an oncogenic mutational mechanism and might accelerate telomere shortening (4,12,13).

Long–Evans Cinnamon (LEC) rats with a genetic deletion in the copper-transporting *Atp7b* gene (14), which is homologous to Wilson's disease gene, exhibit accumulation of large amounts of copper in the liver and spontaneously develop chronic hepatitis, cholangiofibrosis and eventually liver tumor (15–17). Such excessive accumulation of transition metals causes chronic inflammation, characterized by excess production of reactive oxygen species (18), because transition metals interact with physiologically produced reactive oxygen species to catalyze the formation of highly cytotoxic hydroxyl radicals via the Fenton/Haber–Weiss reaction (19). Continuous oxidative stress conditions could be responsible for the pathological processes at play in hepatotumorigenesis (16). Thus, LEC rats could be a useful model to define the multistep mechanisms of hepatotumorigenesis induced by oxidative stress.

To elucidate the molecular mechanisms involved in the multistep hepatotumorigenesis, this study investigated genes that are upregulated in a stepwise manner from the naive liver condition to chronic oxidative stress-induced hepatitis and liver tumor by time-series microarray analysis. The time-dependent gene expression profile should reflect the multistep process of hepatotumorigenesis and identify genes that function specifically in this process. The study also undertook data mining to clarify the impact of candidate genes in the tumor-specific dysregulated gene networks using text-mining technology. These analyses would be helpful not only for a better understanding of the multistep process of liver tumor development but also to identify novel features of known genes and target molecules for treatment.

Materials and methods

Tissue samples

Four-week-old male LEC rats were purchased from Charles River Japan (Yokohama, Japan) and maintained in controlled environments. At 4, 26, 39 and 67 weeks of age, the rats were killed by exsanguination of blood from the abdominal aorta under pentobarbital anesthesia. Paired liver tumor and adjacent non-tumor tissue specimens were obtained from 67-week-old LEC rats (n = 8, Figure 1) that had developed liver tumors. Liver tissues without tumor were obtained from 4-, 26- and 39-week-old LEC rats (n = 6 for each) for analysis of the chronological changes in gene expression profiles. Long–Evans Agouti rats at 67 weeks of age (n = 3), which are wild-type rats, served as the control group (a kind gift from Dr Kozo Matsumoto, Tokushima University, Japan). The Committee for the Care and Use of Laboratory Animals of the Jikei University School of Medicine approved all experimental protocols.

Gene expression analysis

Total RNA was extracted from tissue samples using the RNeasy kit (QIAGEN, Valencia, CA). The RNA integrity was assessed using the Agilent 2100 BioAnalyzer (Agilent Technologies, Palo Alto, CA). A comprehensive gene expression analysis was then performed using 3 μg of total RNA from each sample and the GeneChip® Rat Genome 230 2.0 Array (Affymetrix, Santa Clara, CA) containing 31 099 probe sets, according to the instructions supplied by the manufacturer. To confirm the reproducibility of the results, in the first series of experiments (Figure 1), equivalent amounts of RNA from two pairs randomly selected from eight paired liver tumor and adjacent non-tumor tissue specimens were mixed and analyzed. The average gene expression levels for tumor and non-tumor tissue samples were calculated using the four microarray datasets, respectively. In the following experiments (Figure 1), a mixture of

Abbreviations: HCC, hepatocellular carcinoma; LEC, Long–Evans Cinnamon; RT–PCR, reverse transcription–polymerase chain reaction.

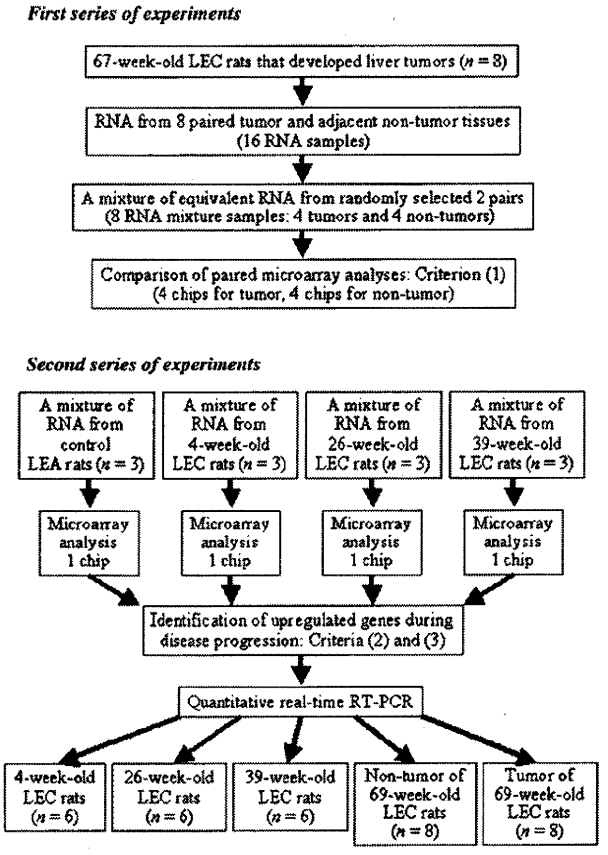

Fig. 1. Analysis flowchart for identification of stepwise upregulated genes during disease progression and multistep hepatotumorigenesis.

equivalent amounts of RNA isolated from LEC rats at 4, 26 and 39 weeks of age and controls (n = 3 for each), respectively, was exploited as an RNA pool for microarray analyses. Microarray datasets were normalized by the robust multi-array analysis, using the R 2.6.1 statistical software together with a BioConductor package (http://www.bioconductor.org/). Normalized expression levels were presented as $\log_2$-transformed values by robust multi-array analysis, and control probe sets were removed for further analysis. To eliminate background signals, genes were selected if their expression was assigned as 'Present' in at least one sample by the GeneChip Operating Software version 1.4 (Affymetrix). A total of 11 305 probes met the quality criteria in the first experiments and were thus subjected to further analysis.

Differential gene expression during disease progression

To identify genes that were upregulated during disease progression and involved in multistep hepatotumorigenesis, each gene was analyzed for fold change and statistical significance using the following three criteria: (i) >2-fold upregulation in tumor tissue samples compared with adjacent non-tumor tissue samples and P values < 0.01 (analyzed by two-tailed, paired t-test); (ii) stepwise increase in relative expression level at weeks 4, 26 and 39, as well as in non-tumor and tumor tissues at week 67 and (iii) relative expression levels at weeks 26 and 39 ('chronic oxidative stress-induced hepatitis phase') and in non-tumor tissue samples higher than the control sample ('no or less oxidative stress status'). The third criterion was important for selection of genes that were considered more strongly influenced by continuous oxidative stress. For paired t-test, false discovery rate was calculated using the Benjamini–Hochberg method. Three similar criteria were applied also to identify downregulated genes: (i) greater than a 2-fold downregulation in tumor tissues compared with adjacent non-tumor tissues and P values < 0.01; (ii) stepwise decrease in relative expression level at weeks 4, 26 and 39, as well as in non-tumor and tumor tissues at week 67 and (iii) relative expression levels at weeks 26 and 39 and in non-tumor tissue samples lower than the control.

Hierarchical clustering

Upregulated and downregulated probe sets were analyzed by hierarchical clustering using the R 2.6.1 statistical software. The gene expression intensities were transformed into Z scores to set the mean expression intensity to 0 and variance to 1 for all genes. Pearson's correlation coefficient was used to calculate a similarity matrix among probe sets. The complete linkage method was used for agglomeration.

Quantitative real-time reverse transcription–polymerase chain reaction

To validate microarray results and to confirm quantitatively any observed differences in gene expression level, each sample was also subjected to reverse transcription–polymerase chain reaction (RT–PCR) and quantitative real-time RT–PCR at least three times using an ABI PRISM 7700 Sequence Detection System (Applied Biosystems, Foster City, CA). Aliquots of RNA were mixed with oligo(dT) primer to obtain complementary DNA using reverse transcriptase. Target genes in the complementary DNA solution were amplified in a PCR mixture containing TaqMan Universal PCR Master Mix (Applied Biosystems), forward and reverse primers and TaqMan probes (Roche Diagnostics, Indianapolis, IN) designed by the Universal Probe Library Assay Design Center (http://www.roche-applied-science.com/sis/rtpcr/upl/adc.jsp). The expression levels of the 18S rat housekeeping gene were also quantified in all samples using the standard primers and TaqMan probe (Applied Biosystems). Differences in gene expression levels among week 4, 26 and 39 samples (n = 6 for each, Figure 1), as well as non-tumor and tumor tissues (n = 8 for both), were examined by one-way analysis of variance followed by Tukey test or Games–Howell procedure, as appropriate. Each dataset was evaluated for normality of distribution by the Shapiro–Wilk test. P values < 0.05 were considered significant. Statistical analyses were performed using the SPSS 17.0 statistical package (SPSS, Chicago, IL).

Immunohistochemistry

Formalin-fixed paraffin-embedded tissue sections were subjected to the streptavidin–biotin–peroxidase complex assay (i-VIEW DAB kit; Ventana Japan, Yokohama, Japan) on the Ventana auto-immunostaining system (Ventana Japan). Slides were pretreated by the recommended procedures for antigen retrieval. The sections were then incubated with rabbit polyclonal and monoclonal antibodies to IQGAP1 (H-109; Santa Cruz Biotechnology, Santa Cruz, CA) and vimentin (Epitomics, Burlingame, CA) at dilutions of 1:500 and 1:200, respectively, for 30 min at room temperature and then washed three times in phosphate-buffered saline. Sections were incubated with the appropriate secondary antibody for 30 min at room temperature.

Western blotting

Liver tissues were homogenized by sonication in lysis buffer. The protein concentration of each tissue lysate was determined using a bicinchoninic acid protein assay kit (Pierce, Rockford, IL). Samples were subjected to sodium dodecyl sulfate–polyacrylamide gel electrophoresis and then electrotransferred onto nitrocellulose membrane. Membranes were blocked with 5% non-fat milk and then probed with the above-described primary antibodies and another for β-actin (Abcam, San Diego, CA). The bound antibodies were visualized with horseradish peroxidase-conjugated secondary antibodies using Enhanced Chemiluminescence western blotting detection reagents (Amersham Pharmacia Biotech, Piscataway, NJ). The substrate reaction was recorded on X-ray film.

Bioinformatics

Pathway analysis was used to clarify the significance of candidate genes in the gene regulatory networks, using GENPAC® (NalaPro Technologies, Tokyo, Japan) and Cytoscape (http://www.cytoscape.org). GENPAC is a novel information extraction system and database for life science using natural language processing/text-mining technology, thereby deducing gene–gene interaction datasets (20). Cytoscape is a visualization and analysis tool for biological pathways (21). Gene ontology annotation was realized by using the GeneCodis 2.0 web tool (http://genecodis.dacya.ucm.es).

Expression of candidate genes in human microarray databases

To determine the expression levels of candidate genes in human liver cancer, we explored and analyzed publicly available microarray datasets of human liver cancer from the National Center for Biotechnology Information Gene Expression Omnibus (GEO: http://www.ncbi.nlm.nih.gov/geo/). For each microarray dataset, differences in the expression levels of candidate genes between human liver cancer and normal liver tissues were examined by Wilcoxon rank-sum test or one-sample t-test, as appropriate.

Results

Stepwise-upregulated genes during the development of liver tumor

Of the 11 305 probe sets filtered, 482 were initially identified as upregulated according to the first criterion of selection. Of these 482 probe sets, 122 met the second criterion. Finally, 87 probe sets (including 22 with no annotation) satisfied the third criterion for

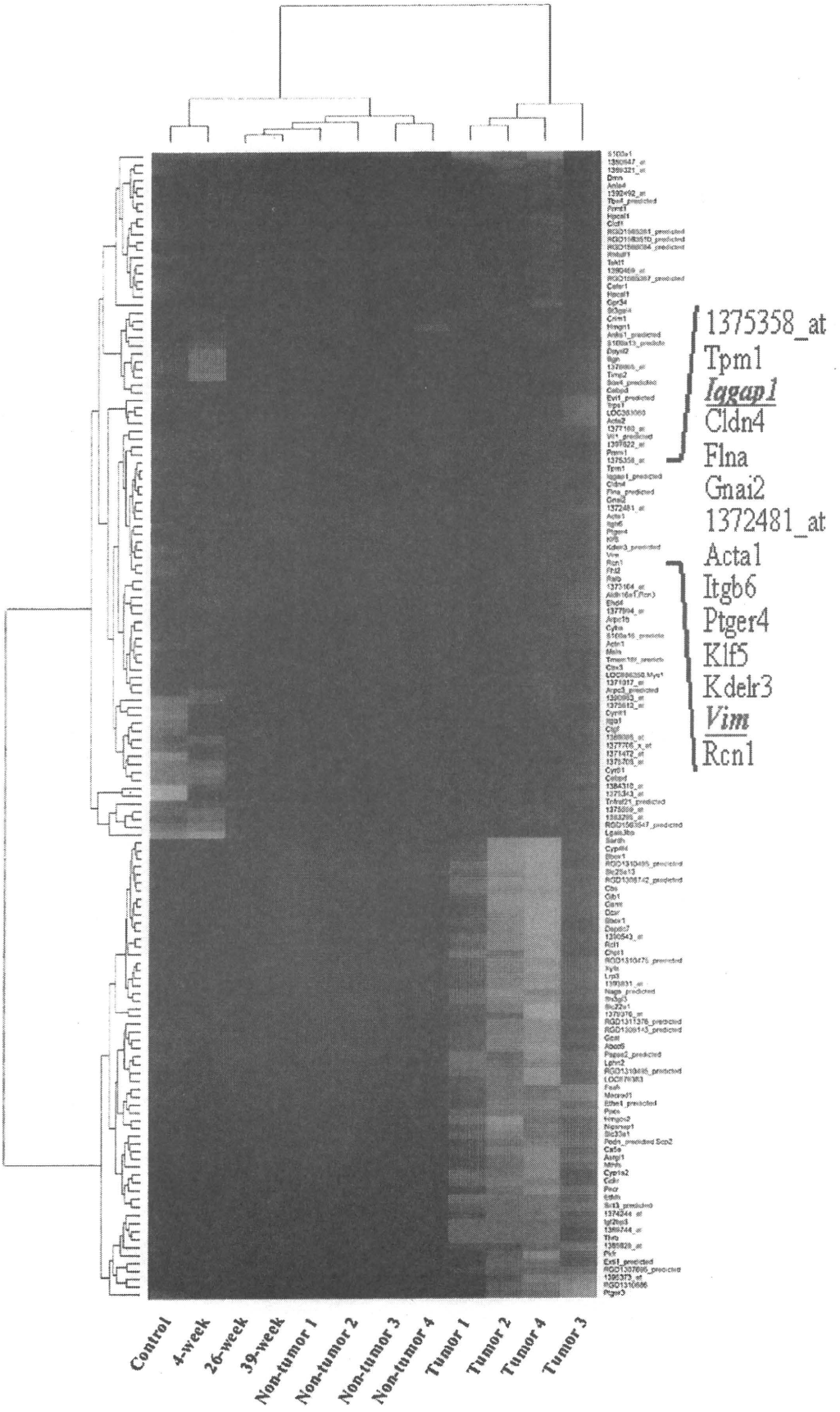
1375358_at
Tpm1
Iqgap1
Cldn4
Flna
Gnai2
1372481_at
Acta1
Itgb6
Ptger4
Klf5
Kdelr3
Vim
Rcn1
Control
4-week
26-week
39-week
Non-tumor 1
Non-tumor 2
Non-tumor 3
Non-tumor 4
Tumor 1
Tumor 2
Tumor 4
Tumor 3

selection (supplementary Table 1 is available at *Carcinogenesis* Online). When the cut-off value for the paired *t*-test for 11 305 probe was set at $P < 0.01$, the estimated false discovery rate was 0.0273. The list contained genes associated with a variety of biological processes, such as cell/cell-matrix adhesion, signal transduction, positive regulation of cell proliferation, integrin-mediated signaling, angiogenesis, regulation of cell growth, positive regulation of the mitogen-activated protein (MAP) kinase kinase kinase cascade, cell motion and inflammatory response. All microarray data have been submitted to Gene Expression Omnibus as GSE17384 ('Gene expression data from the LEC rat model with naturally occurring and oxidative stress-induced liver tumorigenesis'; http://www.ncbi.nlm.nih.gov/geo/). The accession numbers for 'Non-tumor liver at 67 weeks_1 to _4', 'Control liver at 67 weeks', 'Liver at 4, 26 and 39 weeks' and 'Tumor liver at 67 weeks_1 to _4' are GSM434390-3, GSM434394, GSM434395-7 and GSM434398-401, respectively.

Stepwise downregulated genes during the development of liver tumor

Similarly, 58 probe sets (including 7 with no annotation) were identified as being stepwise downregulated during disease progression and tumorigenesis according to all selection criteria (supplementary Table 2 is available at *Carcinogenesis* Online). The list also included genes associated with a variety of molecular functions such as metal/iron ion binding, transferase activity, oxidoreductase activity, protein homodimerization and electron carrier activity.

Two-dimensional hierarchical clustering algorithm

Figure 2 represents the result of hierarchical clustering of the 87 upregulated and 58 downregulated probe sets. A two-dimensional hierarchical clustering algorithm completely distinguished between tumor and non-tumor tissues (Figure 2). The dendrogram shows that samples from 4-week-old LEC and control rats clustered together and formed a statistically different group from samples of 26-, 39- and 67-week-old rats (non-tumor and tumor), indicating that the listed genes were altered by persistent exposure to oxidative stress.

Validation of microarray data by quantitative real-time RT–PCR

To verify the reliability of the microarray data, all the 87 upregulated genes and all time-point samples of each gene were subjected to quantitative real-time RT–PCR. The average mRNA expression levels simply increased in a phased manner in only five genes: connective tissue growth factor (*CTGF*), IQ motif containing GTPase-activating protein 1 (*IQGAP1*), vimentin (*Vim*), smooth muscle alpha-actin (*Acta2*) and reticulocalbin 3 (*Rcn3*). The remaining 82 genes did not show a stepwise increase. Analysis of variance showed significant differences in expression of CTGF, IQGAP1 and vimentin. Finally, *post hoc* analyses showed significant increases in IQGAP1 and vimentin in a stepwise manner during liver disease progression and tumorigenesis (Figure 3). IQGAP1 mRNA levels (mean ± SD) were 0.17 ± 0.15, 0.76 ± 0.21, 1.43 ± 0.49, 2.74 ± 0.34 and 54.33 ± 12.60 in non-tumor liver tissue at week 4, 26, 39 and 67 and tumor tissues, respectively. Similarly, vimentin mRNA levels were 0.0011 ± 0.00035, 0.32 ± 0.08, 0.62 ± 0.28, 4.27 ± 1.92 and 40.78 ± 12.01. All comparisons between two time points except 26 week versus 39 week showed significantly different relative expression levels in both IQGAP1 and vimentin. IQGAP1 and vimentin clustered together and were in the same cluster group (Figure 2).

Immunohistochemical staining and western blot analysis

Next, the expressions of IQGAP1 and vimentin were assessed at the protein level during hepatotumorigenesis by immunohistochemical staining with antibodies against the two proteins (Figure 4A and B). Immunostaining for IQGAP1 and vimentin in the cell membrane or

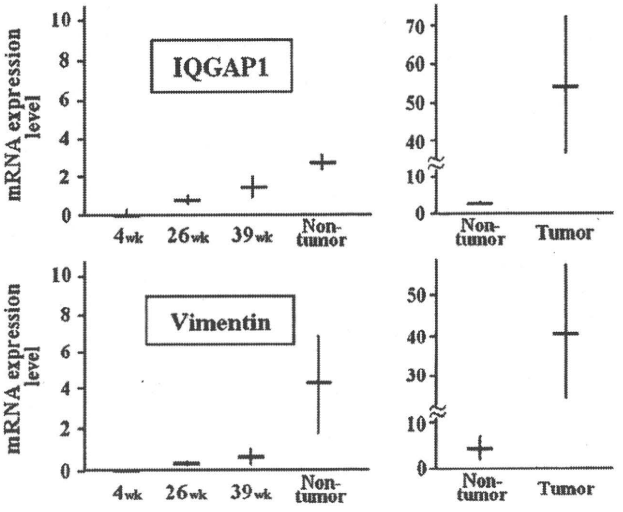

Fig. 3. Validation of differentially expressed genes using quantitative real-time RT–PCR analysis for IQGAP1 and vimentin. One-way analysis of variance and subsequent *post hoc* analyses showed that the expression levels of only two genes, IQGAP1 and vimentin, increased significantly in a stepwise manner during liver disease progression and tumorigenesis. All comparisons between two time points except 26 weeks versus 39 weeks were significantly different in relative expression levels of both IQGAP1 and vimentin ($P < 0.05$).

pericytoplasm gradually increased with time. The cytoplasm of hepatocytes and lymphocytes showed IQGAP1 staining and strongly immunopositive cells were observed in tumor tissues. Western blotting confirmed the immunostaining results for IQGAP1 and vimentin according to the stepwise progression of hepatocarcinogenesis (Figure 4C).

IQGAP1 and vimentin interact with other genes in gene regulatory networks

To provide insights into the relationship of *IQGAP1* and *vimentin* in underlying gene regulatory networks, microarray data and array-independent text mining were integrated by using GENEPAC and Cytoscape. Sixty-five upregulated known functional genes were related to another 470 genes and connected by 1009 interaction edges (supplementary Figure 1 is available at *Carcinogenesis* Online). *IQGAP1* and *vimentin* were identified as important nodes in the network graph and considered as key regulators. Figure 5A extracted from the interactive graph illustrates the direct relationship of *IQGAP1* and *vimentin* with 37 and 18 other regulatory genes, respectively, including *CDH1* (*E-cadherin*) connecting *IQGAP1* and *vimentin*.

We then explored the relationship of these genes to 'oxidative stress'-related, 'carcinogenesis/tumorigenesis'-related or 'fibrogenesis'-related genes. The number of genes that were related to each category and the degree of overlap between gene sets are shown in Figure 5B. Among 38 genes connected directly with *IQGAP1*, 31 and 31 were related to 'oxidative stress' and 'carcinogenesis/tumorigenesis', respectively. Twenty and 8 of 38 genes were associated with both and all categories, respectively. Among 19 genes connected directly with *vimentin*, 15 were related to 'oxidative stress' and 'carcinogenesis/tumorigenesis'. Five of 19 genes were associated with all categories.

IQGAP1 and vimentin in human liver cancer

IQGAP1 and vimentin were significantly upregulated in microarray datasets of human liver cancer (GSE 4108 and GSE14323). In the

Fig. 2. A two-dimensional hierarchical clustering algorithm of gene expression using probe sets for 87 upregulated and 58 downregulated genes. The horizontal and vertical axes of the dendrogram indicate the degree of similarity between genes and liver tissue samples, respectively, as determined by hierarchical clustering. The gene expression changes are presented in graduated color patches from green (least expression) to red (most abundant expression). IQGAP1 and vimentin were classified into the same cluster group. The vertical dendrogram reflects the clinical course during liver disease progression and tumorigenesis.

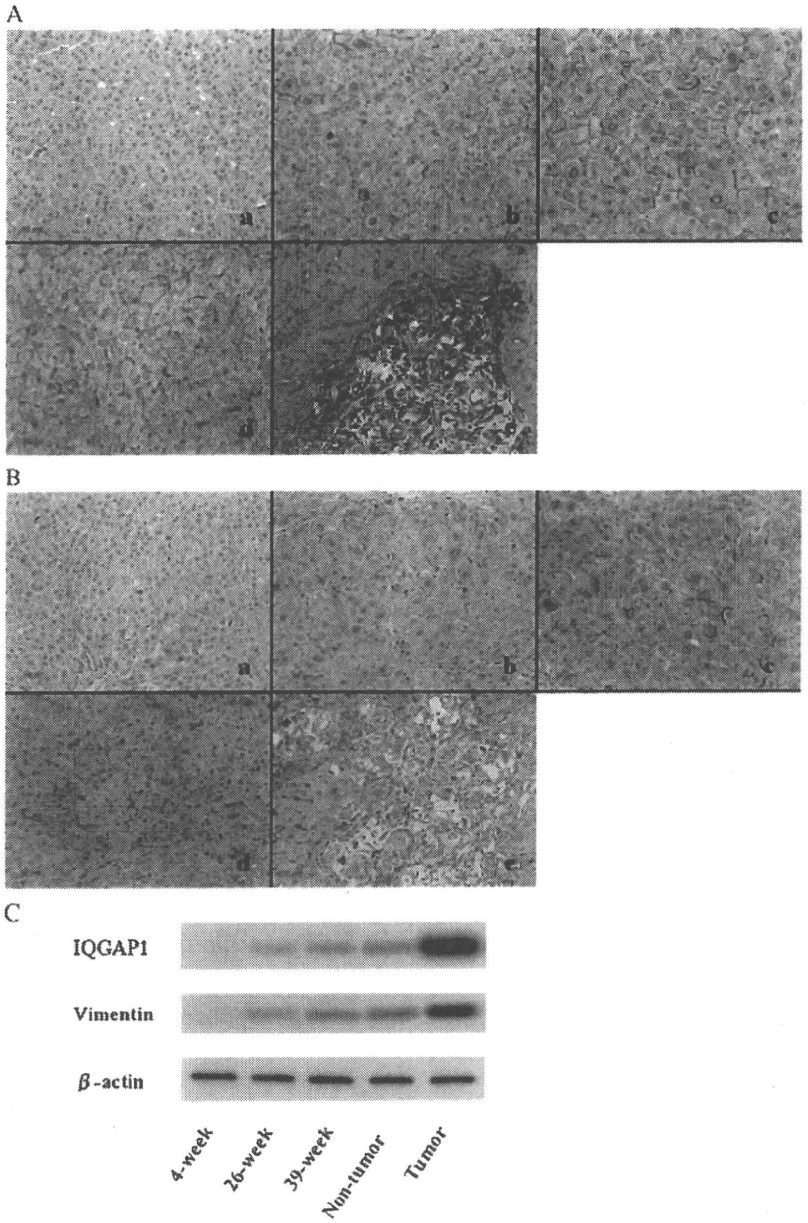

Fig. 4. Immunohistochemical reactivity and western blot analysis of IQGAP1 and vimentin in liver tissue from 4-, 26- and 39-week-old LEC rats (a, b and c), as well as in non-tumor (d) and tumor tissue (e) from 67-week-old LEC rats. (**A**) IQGAP1 staining was prominent at the cell–cell boundaries and cytoplasm according to the stepwise progression of hepatocarcinogenesis. (**B**) Vimentin staining was prominent at the cell–cell boundaries and cytoplasm according to the stepwise progression of hepatocarcinogenesis; bar = 50 μm. (**C**) Western blot analyses. β-Actin was also blotted, as a control. Results are representative data of at least three separate experiments.

GSE4108, the two genes were significantly upregulated in HCC, compared with normal liver tissue ($P = 1.76 \times 10^{-2}$ and 1.69×10^{-6}, respectively; supplementary Figure 2A is available at *Carcinogenesis* Online). In the GSE14323, the two genes were also significantly upregulated in HCC ($P = 7.43 \times 10^{-7}/5.02 \times 10^{-9}$ and 5.97×10^{-14}, respectively; supplementary Figure 2B is available at *Carcinogenesis* Online).

Discussion

To identify specific genes involved in multistep tumorigenesis, multivariate clinicopathological variables should be reduced and simple comparisons between tumor and non-tumor tissues should be avoided. Instead, in the present study, an animal model in which liver tumor developed naturally due to oxidative stress was prepared for microarray analysis to analyze serial changes in gene expression profiles from naive liver status to chronic hepatitis to tumor development. Such conditions or examinations cannot be reproduced or performed in human subjects. The analyses identified IQGAP1 and vimentin as stepwise-upregulated genes throughout the oxidative stress-induced process of hepatotumorigenesis, implicating both as reactive to persistent oxidative stress and important molecules in the mechanism of hepatotumorigenesis. In fact, the GEO database shows that IQGAP1 and vimentin are significantly upregulated in human HCC tissues (GSE4108 and

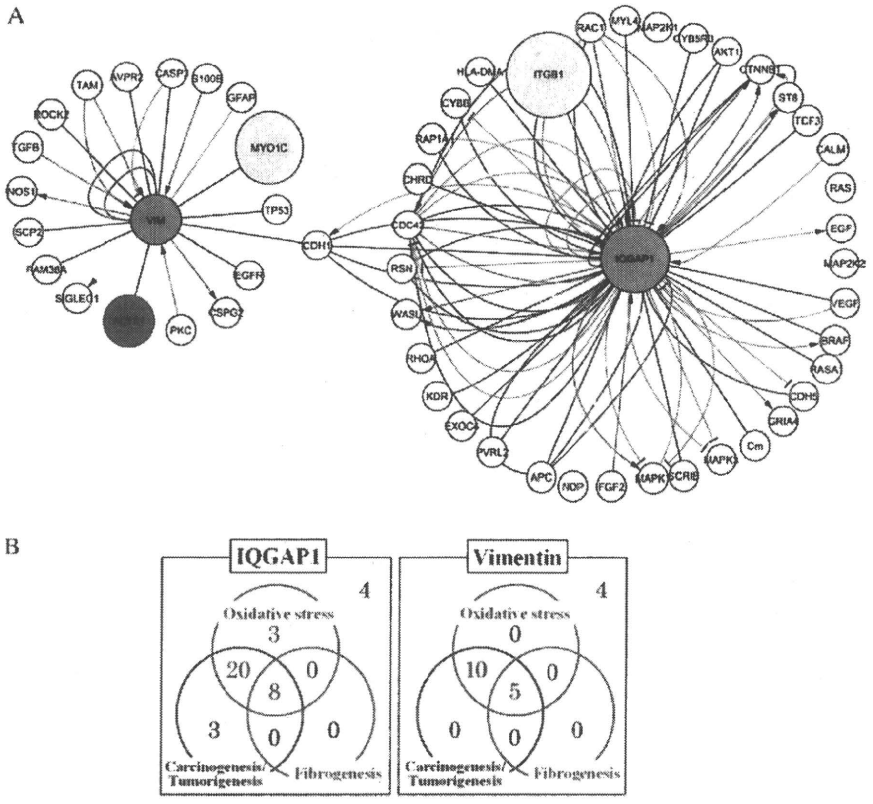

Fig. 5. *IQGAP1*, *vimentin* and related genes. (**A**) Part of the gene regulatory networks for *IQGAP1* and *vimentin*. Microarray data and array-independent text mining were integrated by gene regulatory network analysis (GENPAC). The interaction data were visualized and analyzed by Cytoscape. *CDH1* (*E-cadherin*) is directly linked to both *IQGAP1* and *vimentin*. Color nodes indicate relative overexpression of genes (fold change of tumor to non-tumor) on the microarray data: violet, 4> to ≥2; pale red, 16> to ≥4; red, ≥16 and white, 2> or no data. Node size indicates the proportion of the downstream effectors to the upstream modulators, of which genes are components of various signaling pathways. Edge colors and shapes reflect the interactions between genes: blue, upregulation type, such as 'activate'; red, downregulation type, such as 'inhibit'; green, regulation type, such as 'modulate' without information of up/downregulation; yellow, biochemical type, such as 'phosphorylation' and black, other types, such as 'associate'. (**B**) Biological backgrounds of genes linked directly to *IQGAP1* and *vimentin*. Among 38 genes linked directly to *IQGAP1*, 31 and 31 were related to 'oxidative stress' and 'carcinogenesis/tumorigenesis', respectively. Twenty and 8 of 38 genes were associated with both and all key words, respectively. Among 19 genes connected directly with *vimentin*, 15 were related to 'oxidative stress' and 'carcinogenesis/tumorigenesis'. Five of 19 genes were associated with all categories.

GSE14323, supplementary Figure 2 is available at *Carcinogenesis* Online), relative to other normal liver tissues. This was also confirmed in 165 of our patients with HCC ($P = 1.40 \times 10^{-4}$ and 4.97×10^{-3}, respectively; M.Kaoru and T.Hiroshi, unpublished data).

IQGAP1 is a scaffolding protein that specifically interacts with diverse proteins via multiple motifs. By doing so, IQGAP1 mediates multiprotein complex assembly and regulates multiple physiological cellular processes, such as cell–cell adhesion, cell polarization, cell migration, transcription and regulation of actin cytoskeleton formation and MAP kinase (MAPK) signaling. In addition, many IQGAP1-binding partners are implicated in tumorigenesis and/or tumor progression, including Rac1, Cdc42, Rap1, E-cadherin, β-catenin, components of the MAPK pathway, calmodulin, actin and APC (22–25). IQGAP1 is a downstream effector of Cdc42 and Rac1 (members of the Rho GTPase family). It localizes and interacts with the cytoplasmic domain of E-cadherin (CDH1), β-catenin (CTNNB1) and α-catenin at the cytoplasmic side of adherens junctions to negatively regulate E-cadherin-mediated cell–cell adhesion by interacting with β-catenin and dissociating α-catenin from the cadherin–catenin complex. Activated Cdc42 and Rac1 inhibit IQGAP1, thereby stabilizing the E-cadherin complex link to actin cytoskeleton and ensuring strong and rigid adhesion. Conversely, non-suppressed IQGAP1 results in diminished cell–cell adhesion (22,25,26). In human breast epithelial cells, IQGAP1 contributes to neoplastic transformation, upregulation of cell proliferation, angiogenesis, invasion and high metastatic capacity *in vitro*. Conversely, knockdown of IQGAP1 substantially reduces the amount of active Cdc42 and Rac1 in breast carcinoma *in vivo*. Cdc42/Rac1 and actin participate in IQGAP1-stimulated tumorigenesis, invasion and proliferation (27). In human gastric cancer, the expression levels of Rac1 and IQGAP1 are significantly correlated, while tumors showing E-cadherin mutations have reduced or absent levels of both (28). IQGAP1 also directly interacts with vascular endothelial growth factor type-2 receptor, via which reactive oxygen species derived from Rac1-dependent NAD(P)H oxidase are involved in vascular endothelial growth factor signaling, thereby promoting endothelial cell migration and proliferation that are important for angiogenesis (29). IQGAP1 activates B-Raf to mediate endothelial cell proliferation, which is essential for vascular endothelial growth factor to stimulate angiogenesis (30).

The IQGAP1 gene and/or protein is overexpressed in several human neoplasms: gastric (28,31,32), lung (33), colorectal (34), ovarian (35) and glioblastoma (36). From a clinical aspect, IQGAP1 seems closely associated with tumor invasion and metastasis and with the progression and poor prognosis of malignancies. However, it is not known whether IQGAP1 is the cause or consequence of neoplastic transformation. The present study analyzed the average levels of IQGAP1 mRNA and found increases of >4-fold, >8-fold and >16-fold in non-tumor liver tissues of rats at weeks 26, 39 and 67, respectively, compared with 4-week-old animals (Figure 3). This indicated that IQGAP1 expression was latently upregulated before development of the liver tumor. The immunohistochemical and western blotting results (Figure 4)

further supported that IQGAP1 is positively involved in the process of hepatotumorigenesis. This is the first report to document the stepwise increase of IQGAP1 mRNA and protein expression in a rat model of naturally occurring oxidative stress-induced hepatotumorigenesis. In *Iqgap2*$^{-/-}$ mice, HCC develops in an IQGAP1-dependent manner, while overexpression of IQGAP1 is associated with acquired β-catenin mutations, and dephosphorylated (active) β-catenin accumulates specifically in HCC livers but not in liver tissue from younger wild-type or *Iqgap2*$^{-/-}$ mice without HCC (37).

Vimentin is a cytoplasmic intermediate filament protein synthesized in cells of mesenchymal origin. It is therefore usually expressed in mesenchymal but not epithelial cells, and high vimentin expression in tumor epithelial cells has been correlated with tumorigenic potential, marked by the growth, invasive and migratory ability of cancer cells (38,39). Vimentin knockdown by RNA interference reduces cancer cell activities, resulting in greatly decreased tumorigenic potential (39,40). Reversal of the mesenchymal phenotype by inhibition of vimentin expression restores epithelial characteristics to cells *in vitro* (keratin gene expression) and smaller more differentiated tumors *in vivo* (39). Vimentin expression is also known as a sign of epithelial-to-mesenchymal transition, originally defined as the formation of mesenchymal cells from epithelia during the embryonic stages of development. In this process, the progression of tumors with strong malignant potential requires the epithelial phenotype to be lost along with junctional proteins such as E-cadherin and polarizing of the cells. Meanwhile, the cell acquires a more mesenchymal phenotype with reduced cell–cell adhesion, unpolarized spindle-shaped morphology (fibroblasts and fibroblast-like cells), enhanced cell motility and the presence of mesenchymal cellular markers such as vimentin (41,42).

In fact, advanced liver tumors in LEC rats spread over the liver in a scirrhous growth pattern and sometimes metastasize to lymph nodes. It is noteworthy that the expression levels of vimentin mRNA and protein increased in a stepwise manner during tumorigenesis in this study. Similar to IQGAP1, vimentin was latently upregulated before the development of liver tumors. It also increases in CCl_4-induced cirrhotic mouse livers, whereby hepatocytes derived from such livers and maintained *in vitro* exhibit high expression of vimentin and low expression E-cadherin, with the morphological characteristics of epithelial-to-mesenchymal transition (43). Prolonged exposure of mouse hepatocytes to transforming growth factor-β increases vimentin expression, suggesting that hepatocytes may have fibrogenic potential (44).

The text-mining software used in this study aimed to utilize more comprehensive and recent gene–gene interaction data (http://www.nalapro.com) than manual curation pathway databases, such as Ingenuity Pathway Analysis (45) and MetaCore (46). Moreover, the software provides interaction data with directional information among genes by using natural language processing/text-mining technology, unlike machine curation pathway databases, such as PubGene (47) and BiblioSphere (48), which use a different text-mining algorithm. Bioinformatics, such as integration of additional biological interactive data, is needed to uncover the molecular mechanisms underlying hepatotumorigenesis because the inherently complex and multivariate relations in gene regulatory network lead to difficulties in data interpretation.

In conclusion, IQGAP1 and vimentin were stepwise upregulated in an animal model with naturally occurring and oxidative stress-induced hepatotumorigenesis, implicating both as major molecules initiated and promoted by persistent oxidative stress, as key regulator genes involved in the multistep process of liver tumorigenesis and as targets for the development of novel gene therapies.

Supplementary material

Supplementary Tables 1 and 2 and Figures 1 and 2 can be found at http://carcin.oxfordjournals.org/

Funding

Grant-in-Aid for Scientific Research from the Ministry of Education, Culture, Sports, Science and Technology (Japan) (90322643 to A.T.).

Acknowledgements

We thank Ms Noriko Hashimoto (National Research Institute for Child Health and Development), Ms Mamiko Ohwada, Ms Rie Agata, Ms Yoko Yumoto and Mr Yasuo Mabashi (Jikei University School of Medicine) for the skillful technical assistance.

Conflict of Interest Statement: None declared.

References

1. Obama,K. *et al.* (2005) Genome-wide analysis of gene expression in human intrahepatic cholangiocarcinoma. *Hepatology*, **41**, 1339–1348.
2. Hass,H.G. *et al.* (2008) Identification of osteopontin as the most consistently over-expressed gene in intrahepatic cholangiocarcinoma: detection by oligonucleotide microarray and real-time PCR analysis. *World J. Gastroenterol.*, **14**, 2501–2510.
3. Iizuka,N. *et al.* (2008) Translational microarray systems for outcome prediction of hepatocellular carcinoma. *Cancer Sci.*, **99**, 659–665.
4. Farazi,P.A. *et al.* (2006) Hepatocellular carcinoma pathogenesis: from genes to environment. *Nat. Rev. Cancer*, **6**, 674–687.
5. Blechacz,B. *et al.* (2008) Cholangiocarcinoma: advances in pathogenesis, diagnosis, and treatment. *Hepatology*, **48**, 308–321.
6. Hammill,C.W. *et al.* (2008) Intrahepatic cholangiocarcinoma: a malignancy of increasing importance. *J. Am. Coll. Surg.*, **207**, 594–603.
7. Rosenthal,P. (2008) Hepatocarcinoma in viral and metabolic liver disease. *J. Pediatr. Gastroenterol. Nutr.*, **46**, 370–375.
8. Okabe,H. *et al.* (2001) Genome-wide analysis of gene expression in human hepatocellular carcinomas using cDNA microarray: identification of genes involved in viral carcinogenesis and tumor progression. *Cancer Res.*, **61**, 2129–2137.
9. Iizuka,N. *et al.* (2002) Comparison of gene expression profiles between hepatitis B virus- and hepatitis C virus-infected hepatocellular carcinoma by oligonucleotide microarray data on the basis of a supervised learning method. *Cancer Res.*, **62**, 3939–3944.
10. Schwarz,K.B. (1996) Oxidative stress during viral infection: a review. *Free Radic. Biol. Med.*, **21**, 641–649.
11. Shacter,E. *et al.* (2002) Chronic inflammation and cancer. *Oncology*, **16**, 217–226, 229; (discussion 230–232).
12. Marrogi,A.J. *et al.* (2001) Oxidative stress and p53 mutations in the carcinogenesis of iron overload-associated hepatocellular carcinoma. *J. Natl Cancer Inst.*, **93**, 1652–1655.
13. Kurz,D.J. *et al.* (2004) Chronic oxidative stress compromises telomere integrity and accelerates the onset of senescence in human endothelial cells. *J. Cell Sci.*, **117**, 2417–2426.
14. Wu,J. *et al.* (1994) The LEC rat has a deletion in the copper transporting ATPase gene homologous to the Wilson disease gene. *Nat. Genet.*, **7**, 541–545.
15. Masuda,R. *et al.* (1988) High susceptibility to hepatocellular carcinoma development in LEC rats with hereditary hepatitis. *Jpn. J. Cancer Res.*, **79**, 828–835.
16. Sone,K. *et al.* (1996) Inhibition of hereditary hepatitis and liver tumor development in Long-Evans cinnamon rats by the copper-chelating agent trientine dihydrochloride. *Hepatology*, **23**, 764–770.
17. Meerson,N.R. *et al.* (1998) Identification of B10, an alkaline phosphodiesterase of the apical plasma membrane of hepatocytes and biliary cells, in rat serum: increased levels following bile duct ligation and during the development of cholangiocarcinoma. *Hepatology*, **27**, 563–568.
18. Hensley,K. *et al.* (2000) Reactive oxygen species, cell signaling, and cell injury. *Free Radic. Biol. Med.*, **28**, 1456–1462.
19. Stohs,S.J. *et al.* (1995) Oxidative mechanisms in the toxicity of metal ions. *Free Radic. Biol. Med.*, **18**, 321–336.
20. Kushida,T. *et al.* (2009) *Collection of disease networks by hybrid curation method and the application for pathway analysis.* Proceedings of 2nd International Workshop on Intelligent Informatics in Biology and Medicine, 16–19 March 2009, Fukuoka, Japan, 800–806.
21. Shannon,P. *et al.* (2003) Cytoscape: a software environment for integrated models of biomolecular interaction networks. *Genome Res.*, **13**, 2498–2504.
22. Briggs,M.W. *et al.* (2003) IQGAP proteins are integral components of cytoskeletal regulation. *EMBO Rep.*, **4**, 571–574.
23. Mateer,S.C. (2003) IQGAPs: integrators of the cytoskeleton, cell adhesion machinery, and signaling networks. *Cell Motil. Cytoskeleton*, **55**, 147–155.
24. Noritake,J. *et al.* (2005) IQGAP1: a key regulator of adhesion and migration. *J. Cell Sci.*, **118**, 2085–2092.

25. Brown,M.D. (2006) IQGAP1 in cellular signaling: bridging the GAP. *Trends Cell Biol.*, **16**, 242–249.
26. Kuroda,S. *et al.* (1998) Role of IQGAP1, a target of the small GTPases Cdc42 and Rac1, in regulation of E-cadherin- mediated cell-cell adhesion. *Science*, **281**, 832–835.
27. Jadeski,L. *et al.* (2008) IQGAP1 stimulates proliferation and enhances tumorigenesis of human breast epithelial cells. *J. Biol. Chem.*, **283**, 1008–1017.
28. Walch,A. *et al.* (2008) Combined analysis of Rac1, IQGAP1, Tiam1 and E-cadherin expression in gastric cancer. *Mod. Pathol.*, **21**, 544–552.
29. Yamaoka-Tojo,M. *et al.* (2004) IQGAP1, a novel vascular endothelial growth factor receptor binding protein, is involved in reactive oxygen species—dependent endothelial migration and proliferation. *Circ. Res.*, **95**, 276–283.
30. Meyer,R.D. *et al.* (2008) IQGAP1-dependent signaling pathway regulates endothelial cell proliferation and angiogenesis. *PLoS ONE*, **3**, e3848; (1–11).
31. Sugimoto,N. *et al.* (2001) IQGAP1, a negative regulator of cell-cell adhesion, is upregulated by gene amplification at 15q26 in gastric cancer cell lines HSC39 and 40A. *J. Hum. Genet.*, **46**, 21–25.
32. Takemoto,H. *et al.* (2001) Localization of IQGAP1 is inversely correlated with intercellular adhesion mediated by e-cadherin in gastric cancers. *Int. J. Cancer*, **91**, 783–788.
33. Sun,W. *et al.* (2004) Identification of differentially expressed genes in human lung squamous cell carcinoma using suppression subtractive hybridization. *Cancer Lett.*, **212**, 83–93.
34. Nabeshima,K. *et al.* (2002) Immunohistochemical analysis of IQGAP1 expression in human colorectal carcinomas: its overexpression in carcinomas and association with invasion fronts. *Cancer Lett.*, **176**, 101–109.
35. Dong,P. *et al.* (2006) Overexpression and diffuse expression pattern of IQGAP1 at invasion fronts are independent prognostic parameters in ovarian carcinomas. *Cancer Lett.*, **243**, 120–127.
36. Balenci,L. *et al.* (2006) IQGAP1 protein specifies amplifying cancer cells in glioblastoma multiforme. *Cancer Res.*, **66**, 9074–9082.
37. Schmidt,V.A. *et al.* (2008) Development of hepatocellular carcinoma in Iqgap2-deficient mice is IQGAP1 dependent. *Mol. Cell. Biol.*, **28**, 1489–1502.
38. Bindels,S. *et al.* (2006) Regulation of vimentin by SIP1 in human epithelial breast tumor cells. *Oncogene*, **25**, 4975–4985.
39. Paccione,R.J. *et al.* (2008) Keratin down-regulation in vimentin-positive cancer cells is reversible by vimentin RNA interference, which inhibits growth and motility. *Mol. Cancer Ther.*, **7**, 2894–2903.
40. McInroy,L. *et al.* (2007) Down-regulation of vimentin expression inhibits carcinoma cell migration and adhesion. *Biochem. Biophys. Res. Commun.*, **360**, 109–114.
41. Thiery,J.P. (2002) Epithelial-mesenchymal transitions in tumour progression. *Nat. Rev. Cancer*, **2**, 442–454.
42. Huber,M.A. *et al.* (2005) Molecular requirements for epithelial-mesenchymal transition during tumor progression. *Curr. Opin. Cell Biol.*, **17**, 548–558.
43. Nitta,T. *et al.* (2008) Murine cirrhosis induces hepatocyte epithelial mesenchymal transition and alterations in survival signaling pathways. *Hepatology*, **48**, 909–919.
44. Kaimori,A. *et al.* (2007) Transforming growth factor-beta1 induces an epithelial-to-mesenchymal transition state in mouse hepatocytes *in vitro*. *J. Biol. Chem.*, **282**, 22089–22101.
45. Calvano,S.E. *et al.* (2005) A network-based analysis of systemic inflammation in humans. *Nature*, **437**, 1032–1037.
46. Ekins,S. *et al.* (2007) Pathway mapping tools for analysis of high content data. *Methods Mol. Biol.*, **356**, 319–350.
47. Jenssen,T.K. *et al.* (2001) A literature network of human genes for high-throughput analysis of gene expression. *Nat. Genet.*, **28**, 21–28.
48. Scherf,M. *et al.* (2005) The next generation of literature analysis: integration of genomic analysis into text mining. *Brief. Bioinform.*, **6**, 287–297.

Received April 23, 2009; revised December 7, 2009; accepted December 9, 2009

ELSEVIER

Clinical Imaging 34 (2010) 211–221

CLINICAL IMAGING

Real-time contrast-enhanced ultrasound imaging of focal liver lesions in fatty liver

Guang-Jian Liu[a], Wei Wang[a], Xiao-Yan Xie[a], Hui-Xiong Xu[a], Zuo-Feng Xu[a], Yan-Ling Zheng[a], Jin-Yu Liang[a], Fuminori Moriyasu[b], Ming-De Lu[c,*]

[a]*Department of Medical Ultrasonics, Institute of Diagnostic and Interventional Ultrasound, The First Affiliated Hospital of Sun Yat-Sen University, Guangzhou, China*

[b]*Department of Gastroenterology and Hepatology, Tokyo Medical University, Tokyo, Japan*

[c]*Department of Hepatobiliary Surgery, The First Affiliated Hospital of Sun Yat-Sen University, Guangzhou, China*

Received 20 March 2009; accepted 10 May 2009

Abstract

Purpose: The objective of this study was to investigate the contrast-enhanced ultrasound (CEUS) imaging features of focal liver lesions (FLLs) in fatty liver. **Method:** One hundred FLLs in 98 patients with fatty liver were evaluated with real-time CEUS. **Results:** All malignant FLLs showed hyperenhancement in arterial phase and contrast washout in portal and late phases. Among the FLLs, 3.3% of hemangiomas, 12.5% of focal nodular hyperplasias (FNHs), and 2.5% of focal fatty sparing lesions showed contrast washout in the late phase. The sensitivity and specificity for the characterization of hepatocellular carcinoma, metastasis, hemangioma, FNH, and focal fatty sparing lesions were 100% and 95.6%, 60% and 100%, 93.3% and 98.6%, 87.5% and 97.8%, and 92.6% and 100%, respectively. **Conclusions:** Correct characterization of FLLs in fatty liver by CEUS is possible based on their typical enhancement patterns.

Keywords: Fatty liver; Focal liver lesions; Contrast media; Ultrasound

1. Introduction

Real-time contrast-enhanced ultrasound (CEUS) using second-generation ultrasound contrast agents (UCAs) has been widely used as a noninvasive modality for the detection and characterization of focal liver lesions (FLLs) in clinical practice. The enhancement patterns of different kinds of FLLs on CEUS have been well described in normal liver parenchyma, and the CEUS diagnostic performance of FLLs in normal liver parenchyma has greatly improved compared with conventional gray-scale ultrasound, with 85–96% overall accuracy in differentiating malignant FLLs from benign ones and 81–88.5% overall accuracy in characterizing specific FLLs [1–5].

FLLs in diffuse liver disease such as liver cirrhosis or steatosis are very common in clinical practice. The presence of diffuse liver disease usually makes the appearance of FLLs on baseline gray-scale ultrasound unspecific and greatly increases the difficulty of characterization [6,7]. The CEUS imaging findings and diagnostic performance of FLLs in diffuse liver disease have been rarely reported in large scale at the present time [8–11].

This case series report describes our experience using real-time CEUS with a sulfur hexafluoride (SF6)-filled microbubble UCA in evaluating patients with a variety of FLLs in fatty liver.

2. Materials and methods

2.1. Patients

We retrospectively reviewed the results of conventional and CEUS examinations of 98 patients with FLLs and fatty

* Corresponding author. Department of Hepatobiliary Surgery, The First Affiliated Hospital of Sun Yat-Sen University, 58 Zhongshan Road 2, Guangzhou 510080, People's Republic of China. Tel.: +86 20 87765183; fax: +86 20 87765183.

E-mail address: lumd@21cn.com (M.-D. Lu).

0899-7071/09/$ – see front matter
doi:10.1016/j.clinimag.2009.07.003

liver who were admitted to our hospital between March 2004 and October 2006. The inclusion criteria were as follows: (a) fatty liver background confirmed by typical imaging findings; (b) number of FLLs less than 5; (c) no previously treated lesion; (d) no simple cystic lesion; and (e) diagnosis of FLLs confirmed by histopathology or clinical criteria. There were 59 men and 39 women aged 47.9±13.0 (mean±S.D.) years (range, 20–76 years).

Among these 98 patients, 82 had solitary lesions, 11 had two lesions, and 5 had multiple lesions. Only the most identifiable lesion on baseline gray-scale ultrasound was selected for evaluation with CEUS when a patient had two or multiple lesions. One hepatocellular carcinoma (HCC) patient suffered from twice-distant recurrence after radiofrequency ablation with at least 1-month interval. Thus, a total of 100 FLLs were evaluated in this study. The maximal diameter of the lesions ranged from 1.0 to 11.6 cm (mean, 3.1±1.9 cm), and the depth from the bottom of the lesion to the abdominal wall ranged from 3.5 to 15.0 cm (mean, 6.4±2.3 cm). The final diagnoses were malignant in 17 FLLs and benign in 83 FLLs, including 10 HCCs, 5 metastatic liver cancers (MLCs), 2 intrahepatic cholangiocarcinomas (ICCs), 30 hemangiomas, 8 focal nodular hyperplasias (FNHs), 42 focal fatty sparing lesions, 2 liver abscesses, and 1 solitary necrotic nodule (SNN) (Table 1).

The diagnoses of HCC were all confirmed by histopathology, with the specimens obtained by ultrasound-guided percutaneous biopsy (n=8) or surgery (n=2). Three of the MLC lesions were confirmed by histopathological examination, with the specimens obtained by percutaneous biopsy, and the remaining two lesions were confirmed by clinical data such as history of the primary malignancy, newly detected and continuously enlarged FLLs, and typical imaging findings on contrast-enhanced CT (CECT) or contrast-enhanced MRI [2,3,5]. The metastases were secondary to colorectal carcinoma in two patients, pancreatic carcinoma in two patients, and breast carcinoma in one patient. Both ICCs were confirmed histologically after surgical resection. All hemangiomas and focal fatty sparing lesions were proved by typical findings on CECT or contrast-enhanced MRI and lack of change in lesion size for at least 6 months on imaging follow-up [2,5]. All FNHs, liver abscesses, and SNNs were confirmed by ultrasound-guided percutaneous biopsy or aspiration and imaging follow-up for at least 6 months.

Fatty liver was confirmed by multiple imaging findings, with diagnostic criteria as follows: (a) on ultrasound: bright hepatic parenchyma with echogenicity higher than that of the right renal cortex and poor visualization or nonvisualization of portal vein borders, the diaphragm, or the posterior portion of the right lobe [12]; and (b) on CT: low attenuation of liver parenchyma on unenhanced CT, with values at least 10 HU lower than those of the spleen [13].

2.2. Contrast-enhanced sonography

CEUS examinations were performed with an Acuson Sequoia 512 scanner (Signature 7.2; Siemens Medical Solutions, Mountain View, CA) and a 4V1 vector transducer with frequencies of 1–4 MHz. The CEUS imaging technique and UCA used in the present study were contrast pulse sequencing (CPS) and SF6-filled microbubble contrast agent (SonoVue; Bracco, Milan, Italy), respectively.

Before administration of the UCA, baseline gray-scale ultrasound was performed to scan the entire liver. The imaging settings of the ultrasound scanner were optimized to get the best depiction of the target lesion. Diagnostic information, including the diameter, echogenicity, shape, and margin of each lesion, was recorded. After initiation of CPS imaging mode, a bolus injection of 2.4 ml of UCA was administered through a 20-gauge needle placed in the antecubital vein, followed by a 5-ml flush of 0.9% normal saline solution. Upon completion of the UCA injection, a timer is started simultaneously. The mechanical index (MI) indicated on the screen was between 0.14 and 0.21. The lesion was observed continuously for 6 min on CPS imaging mode. Based on previous literature, arterial phase is defined as 7–30 s after contrast agent injection, portal phase is defined as 31–120 s after contrast agent injection, and late phase is defined as 121–360 s after contrast agent injection [1–5]. The digital cine clips of baseline gray-scale ultrasound and the entire CEUS examination were stored in a hard disk incorporated in the scanner and converted from DICOM files into low compressed AVI files for subse-

Table 1
General features of FLLs (N=100)

Lesion	Lesion size (cm)	Depth (cm)	Number of lesions	Number of male/female patients	Patient age (years)
HCC	3.8±1.2[a] (1.6–5.3)	7.1±2.5[a] (4.4–10.9)	10	8/2	57.6±10.1[a] (41–73)
ICC	5.8, 7.8	6.8, 9.7	2	1/1	52, 60
MLC	3.0±0.6[a] (2.1–3.6)	8.3±1.8[a] (6.0–10.3)	5	2/3	58.0±9.7[a] (41–64)
Hemangioma	3.6±2.5[a] (1.0–11.6)	6.4±2.3[a] (3.5–15.0)	30	18/12	51.5±11.4[a] (34–75)
FNH	2.2±0.6[a] (1.6–2.9)	6.0±1.6[a] (4.0–8.1)	8	4/4	37.3±12.7[a] (24–64)
Focal fatty sparing lesions	2.3±0.9[a] (1.0–5.1)	5.8±1.8[a] (3.5–11.2)	42	25/17	43.1±11.3[a] (20–74)
Abscess	6.0, 9.2	5.5, 14.0	2	2/0	54, 76
SNN	1.7	5.5	1	1/0	28

[a] Data are expressed as mean size±S.D., with ranges indicated in parentheses.